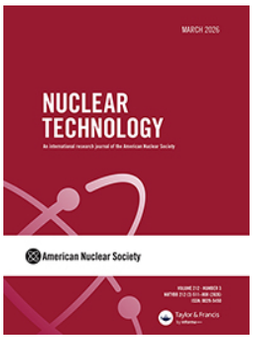

Nuclear Technology

ISSN: 0029-5450 (Print) 1943-7471 (Online) Journal homepage: www.tandfonline.com/journals/unct20

Economic Prospects of Fuel and Outage Costs for Equilibrium Cycles of a Low Power Density PWR-Style SMR

Flavio Ferella, Marcus Seidl , Fausto Franceschini , Cecilia Gustavsson , Henrik Sjöstrand , Andreas Solders & Jesper Kierkegaard

To cite this article: Flavio Ferella, Marcus Seidl , Fausto Franceschini , Cecilia Gustavsson , Henrik Sjöstrand , Andreas Solders & Jesper Kierkegaard (08 Apr 2026): Economic Prospects of Fuel and Outage Costs for Equilibrium Cycles of a Low Power Density PWR-Style SMR, Nuclear Technology, DOI: 10.1080/00295450.2026.2620004

To link to this article: https://doi.org/10.1080/00295450.2026.2620004

Published online: 08 Apr 2026.

NUCLEAR TECHNOLOGY

DOI: https://doi.org/10.1080/00295450.2026.2620004

Review Article

Economic Prospects of Fuel and Outage Costs for Equilibrium Cycles of a Low Power Density PWR-Style SMR

Flavio Ferella [a], Marcus Seidl [b], Fausto Franceschini [c], Cecilia Gustavsson [a], Henrik Sjöstrand [a], Andreas Solders [a], and Jesper Kierkegaard [d]

[a] *Physics and Astronomy, Uppsala University, Uppsala, Sweden;* [b] *Hermann-Von-Helmholtz-Platz 1, Karlsruhe Institute of Technology, Karlsruhe, Germany;* [c] *Westinghouse Mangiarotti Via Timavo, Monfalcone, Italy;* [d] *Westinghouse Electric Sweden, Västerås, Sweden*

Received October 1, 2025
Accepted for Publication January 15, 2026

Abstract — *Small modular reactors (SMRs) have gained attention for their potential to reduce capital investment and enhance deployment flexibility. However, these benefits often come at the cost of reduced neutron economy and efficiency, which could increase the fuel share of the total levelized cost of electricity. This study evaluates the economic performance of a low power density pressurized water reactor–style SMR using the Westinghouse integrated levelized cost of electricity methodology. We investigate the impact of cycle length and core reload fraction on fuel and outage costs for equilibrium cycles. Additionally, a Monte Carlo–based sensitivity analysis is performed to assess the robustness of the results under uncertainty in the economic input parameters. The study also explores the economic viability of adopting low-enriched uranium plus for extended-cycle operation. The results provide insights into fuel utilization and cost optimization strategies for sustainable SMR deployment.*

Keywords — *Levelized cost of electricity (LCOE), small modular reactor (SMR), in-core fuel management, optimization strategies.*

I. INTRODUCTION

The International Atomic Energy Agency (IAEA) Advanced Reactors Information System currently lists more than 100 small modular reactor (SMR) designs under development. From a core design point of view, some of these are scaled-down versions of large [>1000 MW(electric)] light water reactors (LWRs). In some cases, the reduction in electrical output is achieved not only by decreasing the core dimensions, but also by reducing the core power density. This solution allows for cycle length extensions without compromise on the core reload fraction (CRF), and may improve the neutron economy.

This work was conducted on a 121–lattice element Generation III+ (Gen III+) pressurized light water reactor (PWR)–style SMR fueled with a modern 17×17 square lattice fuel design and operating with a core power density of approximately 47 W/cm^3, a relatively low value in comparison to large Gen III+ PWRs such as the AP1000®, which is characterized by a power density of approximately 108 W/cm^3 [1].

In particular, we studied the effect of cycle length and CRF on the economic performance of equilibrium cycles. In addition, for 12-month, 18-month, 24-month, 36-month, and 48-month cycles, using Monte Carlo sampling, we conducted a sensitivity analysis on the economic input parameters to assess the robustness of the results when accounting for the intrinsic uncertainty of the economic input parameters, and we evaluated whether adopting low-enrichment uranium plus (LEU+) offers an economic benefit for operation with long cycles.

CONTACT Flavio Ferella flavio.ferella@physics.uu.se

The levelized cost of electricity (LCOE) associated with fuel and outages was selected as the economic performance indicator, and was evaluated according to the Westinghouse integrated levelized cost of electricity (WILCOE) [2] methodology, implemented in accordance with the INPRO (International Project on Innovative Nuclear Reactor and Fuel Cycles) methodology for sustainability–Economics [3], developed by the IAEA.

One of the objectives of the optimization, and the driving force for this research, was to assess the sustainability of SMRs. In fact, there has been a concern that the potential reduction in the neutron economy of SMRs would lead to increased volumes of high-level waste per unit of energy generated, in comparison with large-scale LWRs [4]. In this context, fuel utilization, defined as the ratio between total thermal output and feed of ^{235}U mass, was selected as a metric to compare the performance of different configurations.

The Westinghouse lattice code PARAGON [5] was chosen to assess the input data for the creation of the linear reactivity model (LRM) [6,7], which was adopted to evaluate the feed batch enrichment required for different cycle lengths and CRF values, thereby allowing for the calculation of the economic indicators.

II. BACKGROUND AND METHODOLOGY

Equilibrium cycles are conditions where the fuel feed inventories and discharge conditions do not change appreciably in successive cycles. While being an idealization of real operating conditions, they are useful for evaluating the long-term fuel cycle cost potential of various fuel management strategies. However, simulating equilibrium cycles is computationally expensive, as it requires repeated application of cycle-to-cycle explicit fuel management schemes. Moreover, this approach lacks flexibility to systematically explore how variations in the cycle length, feed inventories, and average discharge burnup affect economic performance.

An alternative is to use a LRM, which explicitly relates these three parameters. This method enables the efficient analysis of economic performance under different operational scenarios without the computational burden of full equilibrium cycle simulations.

II.A. Linear Reactivity Model

LRMs exploit the lattice reactivity potential to construct a set of state equations for equilibrium cycles. Let k_∞ be the multiplication factor of an infinite lattice, and let ρ represent the reactivity of an infinite fuel assembly (FA) lattice, expressed as

$$\rho = \frac{k_\infty - 1}{k_\infty} . \tag{1}$$

For a PWR, the LRM assumes a linear relationship between the reactivity and the burnup/exposure E. Given a FA lattice with average enrichment e, the polynomial expansion of reactivity as a function of exposure can, with good accuracy, be approximated by its first term over exposure ranges typical of large PWRs,

$$\rho(e,E) \approx \rho_0(e) - \left(\frac{\partial \rho}{\partial E}\right)_e E = \rho_0(e) - A(e)E , \tag{2}$$

where $\rho_0(e)$ represents the initial lattice reactivity. Fig. 1 illustrates the reactivity evolution as a function of burnup/exposure for lattices without burnable absorbers at different enrichments under the assumption of constant power density and constant soluble boron concentration (500 ppm) evaluated using the PARAGON code with critical spectrum (B1) correction. The effect of xenon buildup is evident, producing a sharp drop in lattice reactivity until the equilibrium concentration is reached, typically after about 7 days of operation at constant power density. The linear approximation is shown with dashed lines, where slopes $A(e)$ and intercepts ρ_0 were evaluated according to

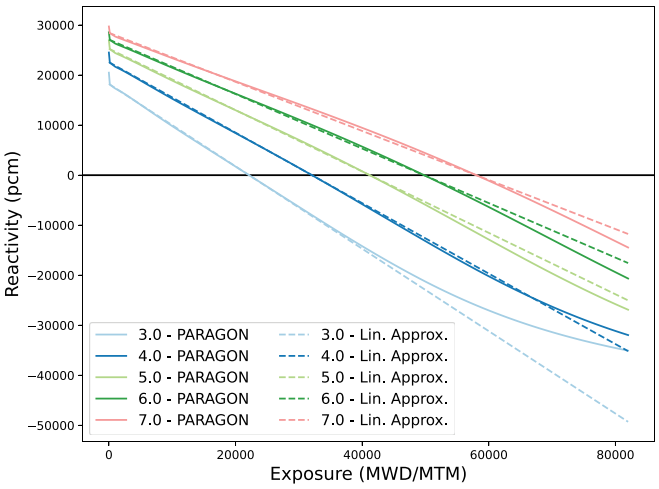

Fig. 1. Comparison of the lattice reactivities evaluated using the lattice code PARAGON and the linear approximation adopted in the LRM formulation as a function of exposure. Different colors represent ^{235}U enrichments ranging from 3.00 to 7.00 wt%.

$$A(e) \equiv \left(\frac{\partial \rho}{\partial E}\right)_e \simeq \frac{\rho_{Xe,eq}(e)}{E(\rho = 0) - E(\rho = \rho_{Xe,eq})} \quad (3)$$

$$\rho_0(e) \simeq \rho_{Xe,eq}(e) + A(e)E(\rho = 0)\,, \quad (4)$$

where $\rho_{Xe,eq}(e)$ and $E(\rho = \rho_{Xe,eq})$ denote, respectively, the reactivity and the exposure at the time step corresponding to the equilibrium xenon concentration, and $E(\rho = 0)$ is the burnup at which zero reactivity is achieved.

This linear approximation was adopted for the construction of the LRM. Although some deviation from the linear trend appears with burnup, originated by spectral and plutonium buildup differences for the various enrichments, the linear fit approximation was deemed acceptable for this application, also considering the enrichment and burnup ranges of practical interest at the equilibrium cycle.

LRM exploits the potential assembly reactivity to characterize the relationship between the enrichment, cycle length T_c, and batch number N in equilibrium cycles. In this context, the batch number represents the average number of irradiation cycles that a FA undergoes before being discharged from the core, and can be evaluated from the number of FAs discharged/introduced at each refueling N_{fresh} and the total number of core fuel assemblies N_{TOT},

$$N = \frac{N_{\text{TOT}}}{N_{\text{fresh}}}\ . \quad (5)$$

In this work, the reciprocal of the batch number, known as the CRF, was also adopted,

$$\text{CRF} = \frac{1}{N} = \frac{N_{\text{fresh}}}{N_{\text{TOT}}}\ . \quad (6)$$

In this work, a uniform core power density was assumed, denoted P_{dens}, and expressed in kilowatts per kilogram of heavy metal (kW/kg HM). Although refined techniques have been developed to account for uneven power sharing [8], the predictions obtained assuming constant power density did not differ by more than 5% with respect to detailed calculations in this case. In addition, in accordance with the theoretical foundation of LRM, this work was conducted assuming lattices without burnable absorbers, without control rods, and assuming a constant middle-of-cycle soluble boron concentration.

These assumptions introduce some biases compared to the core behavior with actual geometry and detailed fuel management. For example, in low-leakage loading patterns, the periphery of the core is typically filled with high-burnup fuel, reducing neutron leakage at the expense of increased power peaking. Concurrently, burnable absorbers provide a strong negative reactivity contribution at the beginning of the cycle, substantially modifying the reactivity evolution from the linear trend and potentially reducing cycle length [9]. The negative reactivity introduced by burnable absorbers is particularly pronounced in equilibrium conditions with high CRF or in long cycles with high feed enrichment, where larger concentrations of burnable absorbers are required to comply with design criteria and avoid excessive soluble boron concentrations.

To restore consistency between realistic full-core calculations and lattice-level calculations, a reactivity penalty factor ρ_P was introduced. This factor compensates for effects related to leakage and residual burnable absorbers at end of cycle. The value was fine-tuned to provide enrichment estimates within a tolerance of 0.2 wt % compared to detailed fuel management schemes for some selected core designs, used as reference across a range of cycle lengths and CRFs. This penalty factor was subtracted from the initial reactivity to generate the reactivity data set used for constructing the LRM,

$$\rho_0^{\text{LRM}}(e) = \rho_0(e) - \rho_P\ . \quad (7)$$

A lattice reactivity database was developed considering a modern 17×17 square lattice fuel design with ^{235}U enrichment ranging from 2.50 to 7.00 wt% in increments of 0.25 wt%. Lattice depletion calculations were performed assuming a fixed soluble boron concentration of 500 ppm using the PARAGON code.

Table 1 reports the core properties and FA lattice design, while Table 2 summarizes the initial reactivities and slopes adopted for the construction of the LRM for different enrichments.

In accordance with the theoretical foundations presented in Ref. [6], under the hypothesis of constant power density at each cycle of irradiation of length T_c, expressed in effective full power days (EFPDs), exposure for each FA increases by a factor,

TABLE 1

Core and Lattice Parameters Adopted for the Construction of the LRM and the Evaluation of Reactivity Data

Parameter	Value
P_{dens} (kW/kg HM)	17.64
N_{TOT}	121
Reference FA design	PRIME$^{\text{TM}}$ RFA-II lattice
Active core height (cm)	≈366.0
ρ_P (pcm)	2800

TABLE 2

Database of Reactivity Data, Including Initial Reactivities and Slopes Used in the LRM Formulation and the Reactivity Values Derived from the Penalty Factor

Enrichment (wt%)	$\rho_0(e)$ (pcm)	$\rho_0^{\mathrm{LRM}}(e)$ (pcm)	$A(e)$ (pcm/(MWd/kg HM))
2.50	14 828	12 028	885
2.75	16 678	13 878	856
3.00	18 232	15 432	823
3.25	19 559	16 759	791
3.50	20 705	17 905	761
3.75	21 705	18 905	731
4.00	22 587	19 787	704
4.25	23 369	20 569	679
4.50	24 071	21 271	656
4.75	24 701	21 901	634
5.00	25 273	22 473	613
5.25	25 793	22 993	594
5.50	26 270	23 470	577
5.75	26 706	23 906	561
6.00	27 110	24 310	545
6.25	27 483	24 683	530
6.50	27 829	25 029	516
6.75	28 153	25 353	503
7.00	28 454	25 654	490

$$E_c(N,e) = P_{dens}T_c(N,e) = \frac{\rho_0^{\mathrm{LRM}}(e)}{A(e)}\frac{2N}{N(2N+1-N)}\ , \tag{8}$$

where $\lceil\cdot\rceil$ represents the ceiling operator, introduced to account for the discontinuities in the fuel residence time when the batch number assumes nonintegral values. Rearranging Eq. (8) to isolate the cycle length allows for its estimation based on the batch number and the average batch enrichment,

$$T_c = \frac{E_c}{P_{dens}} = \frac{1}{P_{dens}}\frac{\rho_0^{\mathrm{LRM}}(e)}{A(e)}\frac{2N}{N(2N+1-N)}\ . \tag{9}$$

The average discharge burnup B_d, expressed in megawatt-days per kilogram of heavy metal (MWd/kg HM), can also be evaluated starting from Eq. (8), as on average each FA resides in the core for N cycles,

$$B_d(N,e) = NP_{dens}T_c = \frac{\rho_0^{\mathrm{LRM}}(e)}{A(e)}\frac{2N^2}{N(2N+1-N)}\ . \tag{10}$$

This quantity is fundamental in order to evaluate the total energy produced by each FA, which affects the total electrical output, and considering the waste fees associated with the total electrical output, the spent fuel cost.

The results of the LRM applied to the reactor core under examination are presented in Fig. 2. In particular, we evaluated the cycle length and average discharge burnup as follows:

1. Fixing N and varying the enrichment to highlight equilibrium cycles characterized by equal CRF (blue in Fig. 2).

2. Fixing the enrichment and varying the CRF to highlight the equilibrium cycles with equal average batch enrichment (green in Fig. 2). In particular, derivative discontinuities occur at integer values of N caused by abrupt changes in $\lceil N\rceil$ caused by the ceiling function.

Fig. 2 provides insights into the economic performance at the equilibrium cycle when it is coupled with an economic model, as it shows the relationship connecting feed inventories to operational parameters and discharge conditions.

II.B. WILCOE Methodology and Economic Input Parameters

The WILCOE methodology was applied to quantify the contributions of fuel and outage components to the LCOE.

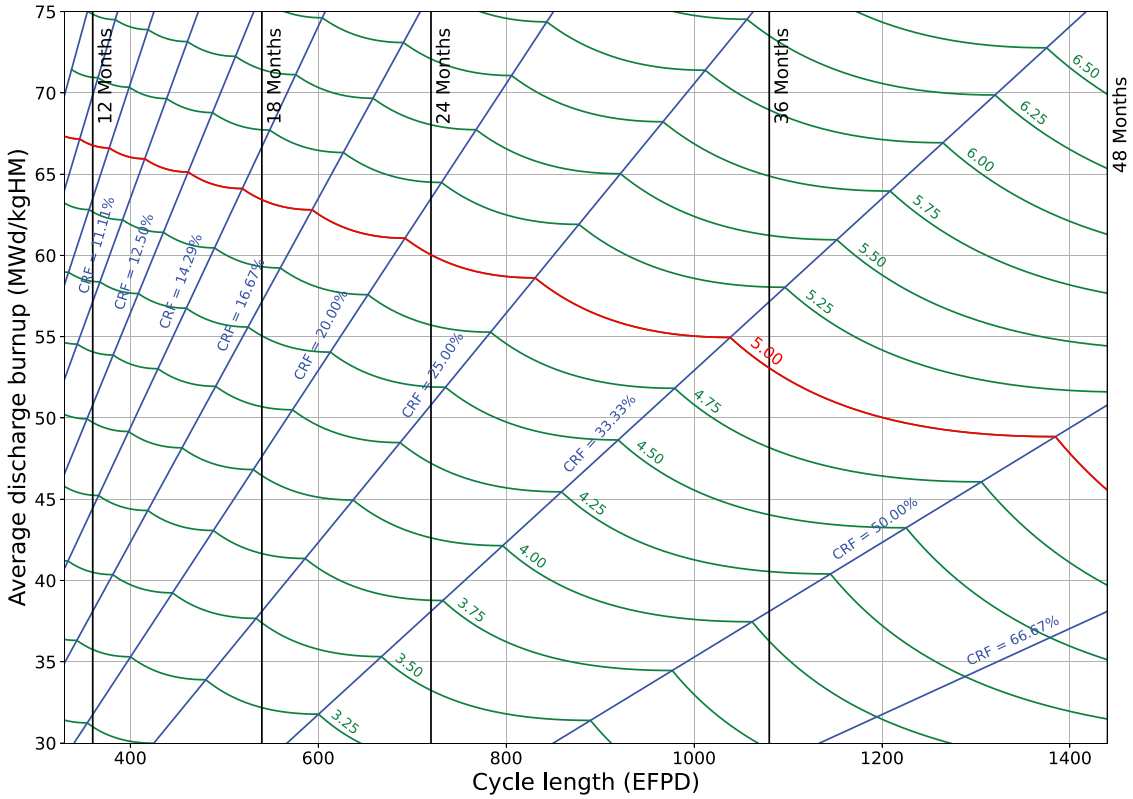

Fig. 2. Relationship between batch enrichment, CRF, cycle length, and average discharge burnup in equilibrium cycles for the selected reactor. In particular, the equilibrium cycles characterized by equal CRFs (blue) and equal batch enrichment (green) are highlighted. In addition, the current regulatory limit for the fuel enrichment (red) is reported.

In this approach, the fuel- and outage-related LCOE for equilibrium cycles is computed using a comprehensive cash flow model that encompasses all activities, from uranium ore procurement to spent fuel disposal,

$$\mathrm{LCOE} = \frac{C_{\mathrm{fuel}} + C_{\mathrm{preop}} + C_{\mathrm{op}} + C_{\mathrm{outages}} + C_{\mathrm{sf}}}{\mathrm{MWh(electric)}} \quad [\$/MWh]\,, \tag{11}$$

where all cost components are expressed in 2035 U.S. dollars through inflation adjustment.

In the initial phase, a systematic evaluation of LCOE trends and fuel utilization was performed across a broad range of configurations, varying the number of batches and cycle lengths under fixed economic input parameters. Specifically, for LCOE estimation, four economic scenarios were defined:

1. *Favorable scenario*: Economic input data providing the lower bound of the LCOE distribution.

2. *Baseline scenario*: Economic input data set to average or most probable values.

3. *Unfavorable scenario*: Economic input data providing the upper bound of the LCOE distribution.

4. *Extended-outage scenario*: Baseline economic input data with additional outage penalties for cycle lengths exceeding 24 months.

Within this framework, we established fixed parameters for N and enrichment while evaluating the cycle length and average discharge burnup. The evaluation of N was based on increments of the reload batch size, ranging from one FA per quadrant to simultaneous refueling of the entire core.

Subsequently, a sensitivity analysis was conducted on economic assumptions. A local sensitivity analysis was first performed to quantify the marginal impact of incremental changes in the individual economic parameters. Additionally, a global sensitivity analysis based on Monte Carlo sampling was employed to compare the economic performance of cycles with lengths of 12 months, 18 months, 24 months, 36 months, and 48 months under stochastic variations of the economic input data.

II.B.1. Cost Breakdown: Fuel Costs

The fuel cost C_{fuel} encompasses all expenses associated with the nuclear fuel cycle stages: uranium ore procurement, purification, conversion to UF_6, enrichment, and fuel fabrication. These costs are derived from the required UO_2 feed inventories, and ultimately, from the corresponding quantities of ore (U_3O_8), separative work units (SWUs), and heavy metal (HM). Manufacturing-related costs are aggregated into a single term proportional to the total HM mass.

The overall fuel cost is expressed as

$$C_{\text{fuel}} = m_{ore}(f \cdot C_{ore} + C_{conv}) + W_{\text{SWU}} C_{\text{SWU}} + m_{\text{HM}} C_{fabr}[\$] , \quad (12)$$

where C_{ore} is the ore cost (\$/lb), C_{conv} is the conversion and purification costs (\$/kg), C_{SWU} is the SWU cost (\$/kg) adopted to quantify the enrichment expenses, and C_{fabr} are the fabrication costs (\$/kg), and where f (approximately 2.6) is a factor that accounts for both the unit conversion from kilograms to pounds and the uranium mass fraction in U_3O_8.

Let m_{UO_2} denote the UO_2 feed mass (in kilograms) and $|e|$ the average enrichment of the batch (in wt%). The HM mass can be obtained from the uranium mass fraction in UO_2 x_{U} as

$$m_{\text{HM}} = x_{\text{U}} m_{UO_2}(\text{kg}) . \quad (13)$$

The SWU requirement and U_3O_8 inventory are determined using the feed-to-product ratio (ftp),

$$R_{ftp} = \frac{|e| - e_{tails}}{e_{nat} - e_{tails}} . \quad (14)$$

Accordingly,

$$W_{\text{SWU}} = m_{\text{HM}} [V(|e|) - V(e_{nat}) - R_{ftp}(V(e_{nat}) - V(e_{tails}))](\text{kg}) \quad (15)$$

and

$$m_{ore} = m_{\text{HM}} \cdot \frac{R_{ftp}}{\eta_{conv}}(\text{kg}) , \quad (16)$$

where $V(x)$ denotes the value function [10], η_{conv} is the conversion efficiency, and e_{nat} and e_{tails} represent the natural uranium enrichment and the enrichment of the tails, respectively.

The input data adopted for the fuel cost estimation are reported in Tables 3 and 4. The assumptions adopted in this study are based on 2017 nuclear fuel cost projections [11]. These projections integrate expert judgment and documented trends in price escalation.

It is important to note that the analysis was conducted under the assumption that once commercial capabilities for LEU+ fuel (e.g., fuel with ^{235}U enrichment in the 5% to 10% range) are established, the fabrication costs and enrichment costs per separative work unit C_{SWU} will be the same for LEU+ fuels as for LEU fuels. This assumption was adopted to eliminate any bias in the fuel supply cost differences in the comparison between LEU and LEU+ fuel cycles.

II.B.2. Cost Breakdown: Pre-Operational and Operational Carrying Charges

The term C_{preop} represents the pre-operational carrying charges, i.e., the interest accrued on the previously incurred expenses from the time each operation is executed until the start of the fuel cycle, assuming daily compounding. This cost is calculated as

$$C_{\text{preop}} = \sum_j C_j \left[\left(1 + \frac{I_{\text{pre\_op,eff}}}{365.25} \right)^{-t_j} - 1 \right] , \quad (17)$$

where C_j is the cost (\$) of the j'th operation (e.g., ore acquisition, conversion, enrichment, fabrication), and t_j is the timing of the j'th operation with respect to cycle startup, expressed in days.

TABLE 3

Economic Input Data Adopted for Fuel Cost Estimate: Cost and Timing of the Different Operations, Referred with Respect to Fuel Loading

Operation	Cost (Low)	Cost (Mid)	Cost (High)	Distribution	Timing
Ore acquisition (\$/lb)	66	88	100	Triangular	−18 months
Conversion (\$/kg)	44	55	66	Uniform	−14 months
Enrichment (\$/kg)	138	188	220	Triangular	−9 months
Fabrication (\$/kg HM)	400	500	600	Uniform	−6 months

TABLE 4

Economic Input Data for Fuel Cost Estimate: Inventories and Tails Specification

Parameter	Value
m_{HM} (kg)	464.0
η_{conv} (%)	99.5
$\lvert e \rvert$ (wt%)	2.50 to 7.00
e_{tails} (wt%)	0.165

The effective annual pre-operational interest rate, corrected for inflation, is given by

$$I_{\mathrm{pre\_op,eff}} = \frac{1 + I_{\mathrm{pre\_op}}}{1 + r} - 1 \,, \tag{18}$$

where $I_{\mathrm{pre\_op}}$ is the nominal annual pre-operational interest rate, and R is the annual inflation rate.

The term C_{op} denotes the operational carrying charges, which correspond to the financial costs of immobilizing an asset (e.g., the fuel) in the core while it is being used. These charges are evaluated using a burnup-based depreciation model. Starting from the initial asset value of the fuel, defined as

$$\text{Fuel Value} = C_{\mathrm{fuel}} + C_{\mathrm{preop}} \,,$$

a daily discount rate proportional to the energy produced by the batch of fuel is applied throughout the entire core residence time. The carrying charges are then accrued based on the depreciated fuel asset multiplied by the effective fuel return on investment (ROI), e.g., the fuel ROI adjusted for inflation.

The economic input data selected for the modeling of pre-operational and operational carrying charges are reported in Table 5, where ROI_{fuel} denotes the ROI of fuel. This analysis was conducted under the assumption of a constant ROI, pre-operational interest rates, and inflation rates.

A comprehensive description of the methodology used to evaluate both pre-operational and operational carrying charges can be found in the referenced documentation in Ref. [2].

II.B.3. Cost Breakdown: Outages

The outage-related component of the total cost must be considered when assessing the economic performance of different cycle lengths. In this work, a simplified approach is adopted, where daily outage costs consist of two elements:

TABLE 5

Interest and Inflation Rates Adopted to Model Pre-Operational and Operational Carrying Charges

Parameter	Annual Rate
$I_{\mathrm{pre\_op}}$	0.08
r	0.02
ROI_{fuel}	0.1

1. *Labor costs*: Additional personnel required for refueling and maintenance activities, estimated using a fixed number of labor hours h_{labor} (h/day) paid at an average rate C_{labor} (\$/h).

2. *Replacement energy costs*: The cost of replacing the lost electrical output [MWh(electric)] with alternative energy sources charged at a fixed rate $C_{\mathrm{ele,r}}$ (\$/MWh). In particular for this work, the replacement energy cost represents the difference in wholesale market prices when substituting nuclear generation with higher-cost sources like gas or coal.

Let T_{outage} denote the outage length in days. The total outage cost is then expressed as

$$C_{\mathrm{outages}} = T_{outage} \cdot \left(24 \cdot P_{\mathrm{ele}} \cdot C_{\mathrm{ele,r}} + h_{\mathrm{labor}} \cdot C_{\mathrm{labor}}\right) , \tag{19}$$

where P_{ele} is the plant electrical power output in megawatts.

The economic input data adopted for modeling outages are reported in Table 6. In this analysis, additional labor requirements were estimated to account for approximately 300 to 600 temporary workers engaged in outage operations, assuming an average occupational schedule of 8 h per day. The average hourly wage for these workers was assumed to be three to four times higher than that of current U.S. nuclear reactor operators, as reported by the U.S. Bureau of Labor Statistics[a].

The energy replacement cost estimates in this study integrated a suite of forward-looking, region-specific considerations. These included 2030 projections for the U.S. fleet of large reactors [12], recent surges in global energy prices, and structural features unique to the European energy market. The distribution bounds encompassed plausible extremes driven by anticipated volatility across both the U.S. and European markets under the

[a] https://www.bls.gov/oes/current/oes518011.htm

TABLE 6

Economic Input Data for Outage Modeling

Parameter	Low	Mid	High	Distribution
T_{outage} short outages (days)		20		
T_{outage} long outages (days)		30		
h_{labor} (h/day)	2400	3600	4800	Uniform
C_{labor} ($/h)	150	175	200	Uniform
P_{ele} (MW)		300.0		
$C_{\text{ele,r}}$ ($/MWh)	30.0	60.0	120.0	Triangular

assumption of a low energy demand scenario, considered to represent an optimized outage scheduling strategy.

Regarding the outage duration, two scenarios were considered. Current regulations for large reactors require that the interval between inspections must not exceed 24 months [13]. In the first scenario, a fixed (20-day) outage length was adopted, independent of the cycle length. In the second scenario, the outage length was extended by 10 days whenever the cycle length exceeded the 24-month threshold. This adjustment simulated an intermediate inspection or maintenance activity between two refueling operations, ensuring compliance with existing maintenance frequency requirements (noting that regulations for SMRs may differ from those for large reactors). These two scenarios, illustrated in Fig. 3, report the availabilities for different cycle lengths and for different outage lengths.

II.B.4. Cost Breakdown: Spent Fuel

Assigning an economic indicator to spent fuel management involves a variety of factors. Most countries do not have a legal framework or established solutions for the final disposal, and in addition, each country has specific regulations concerning temporary storage. However, it is standard procedure to move the spent fuel of LWRs into the spent fuel pool for several years before a temporary or permanent solution is applied. In this work, the spent fuel costs have been modeled to account for the following:

1. A transition into the spent fuel pool for 120 months.

2. Fees proportional to the electrical energy output $C_{tax,ele}$ and to the HM mass $C_{tax,\text{HM}}$.

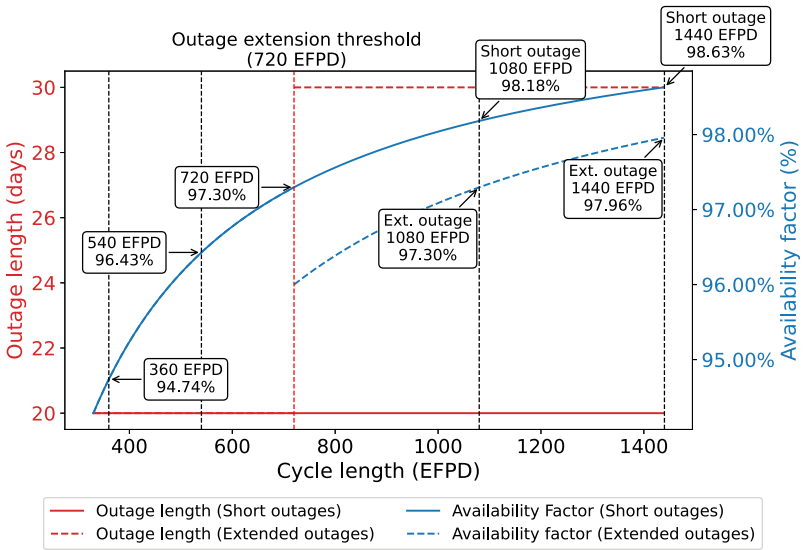

Fig. 3. Outage length and availability factor for two maintenance strategies: short outages, where intervals between maintenance outages is extended beyond current regulations, and extended outages, where a penalty of 10 additional outage days is applied for cycle lengths exceeding 24 months, in accordance with LWR current regulatory requirements. The availability factor for the selected cycle lengths has been highlighted to illustrate the impact of outage duration on plant performance.

3. Transition to dry cask. In this context, we applied a fee proportional to the total number of FAs replaced at each equilibrium core $C_{tax,\mathrm{FA}}$.

4. Interest accrued during these phases.

To summarize, let $T_{cooling}$ denote the cooling time, the spent fuel costs are

$$C_{\mathrm{sf}} = \left(N_{fresh}C_{tax,\mathrm{FA}} + m_{\mathrm{HM}}C_{tax,\mathrm{HM}}\right)\left(1+\frac{\mathrm{ROI}_{\mathrm{eff},fuel}}{365.25}\right)^{-A_1} + \mathrm{MWh(electric)}\left(1+\frac{\mathrm{ROI}_{\mathrm{eff},fuel}}{365.25}\right)^{-A_2}, \tag{20}$$

where A_1 is the total number of days from fuel loading to transition to dry casks,

$$A_1 = N\left(T_c + T_{outage}\right) + T_{cooling} \tag{21}$$

and A_2 is the in-core fuel residence time. The input parameters to model the spent fuel costs are reported in Table 7. In this context, the U.S. market was adopted as the baseline [14], and the proposed distributions reflect potential changes in the legal framework.

II.C. Local and Global Sensitivity Analysis

Two distinct sensitivity analysis methodologies were implemented. The first approach employed a local sensitivity analysis based on a centered finite-difference approximation. For each economic input parameter, a baseline scenario was defined by assigning all parameters either their expected (mean) value or the most probable value from their respective probability distributions.

Subsequently, two perturbed scenarios were generated by setting the selected parameter to its upper and lower bounds, while maintaining all other parameters at their baseline values. The partial derivative of the LCOE with respect to the selected parameter was then estimated as

$$\left(\frac{\partial \mathrm{LCOE}}{\partial C_i}\right)_{\mathrm{baseline}} \approx \left(\frac{(\mathrm{LCOE})^{C_i^{\mathrm{high}}} - (\mathrm{LCOE})^{C_i^{\mathrm{low}}}}{C_i^{\mathrm{high}} - C_i^{\mathrm{low}}}\right)_{C_{j,j\neq i}^{\mathrm{mid}}}. \tag{22}$$

This derivative was subsequently used to quantify the marginal impact of a 10% increase in the corresponding cost component.

The second methodology consisted of a global sensitivity analysis using Monte Carlo simulation. Each economic input parameter was independently sampled 10 000 times according to its prescribed probability distribution, thereby generating 10 000 distinct economic scenarios. For each cycle length, after selecting a reference scenario in terms of the enrichment/CRF, the normalized LCOE for the j'th CRF under the i'th economic scenario was computed as

$$\widehat{\mathrm{LCOE}}_{i,j} = \frac{\mathrm{LCOE}_{i,j}}{\mathrm{LCOE}_{i,\mathrm{ref}}}. \tag{23}$$

This framework enables the assessment of parameter uncertainty propagation and the identification of dominant cost drivers under stochastic conditions.

III. RESULTS

In this section, we discuss the outcomes of the study. We begin by examining the general trends in economic performance and fuel utilization for different cycle lengths and CRFs. Subsequently, we present the results of the global and local sensitivity studies.

III.A. Economic Performance Trends

The economic performance trends for the favorable, baseline, and unfavorable economic input parameters are

TABLE 7

Economic Input Data Adopted for Spent Fuel Modeling

Parameter	Low	Mid	High	Distribution
$C_{tax,ele}$ ($/MWh)	0.0	1.0	2.0	Uniform
$C_{tax,\mathrm{HM}}$ ($/kg HM)	1 000	1 500	2 000	Uniform
$C_{tax,\mathrm{FA}}$ ($/FA)	50 000	75 000	100 000	Uniform
$T_{cooling}$ (Days)		3 600		

presented in Figs. 4, 5, and 6. These figures enable a detailed examination of the influence of the cycle length, CRF, and batch enrichment on the overall economics, allowing for the identification of dominant cost components and the prioritization of optimization efforts. Given that the timeline for LEU+ commercialization aligns with the projected SMR deployment scenarios, it is appropriate to also assess the operational and economic implications of adopting LEU+ as a potential reload fuel.

We first analyze economic performance under fixed discharge burnup conditions (horizontal lines in Figs. 4, 5, and 6), corresponding to a constant average fuel residence time. For small CRFs and shorter cycle lengths, the dominant factor was loss of availability, as illustrated in Fig. 3. However, the trend is nonmonotonic: as CRF increases, an optimum region emerges, beyond which further extensions degrade performance. This behavior indicates that, for longer cycles, fuel costs become increasingly significant, offsetting the benefits of higher availability. These observations remain valid when batch enrichment is fixed and CRF is varied.

When cycle length is held constant (vertical lines), reducing CRF consistently improves the economics within the examined range. This suggests that fuel-related expenses dominate over carrying charges and outage costs, and that the savings from the reduced feed inventory outweighs the extra costs from the increase in batch enrichment for a given cycle length.

For a fixed CRF (oblique lines), where feed HM mass remains constant, the economics improve with increasing cycle length despite higher enrichment requirements. This implies that availability gains outweigh additional fuel costs for a given CRF.

Regarding the optimum region, as economic assumptions shift toward unfavorable scenarios, the optimum shifts toward higher burnup and higher CRF. Two key phenomena were observed:

1. The optimum point moves toward higher burnup, increasing the importance of LEU+ fuel. Implementation of LEU+ fuel, therefore, could yield substantial economic benefits, noting that qualification of

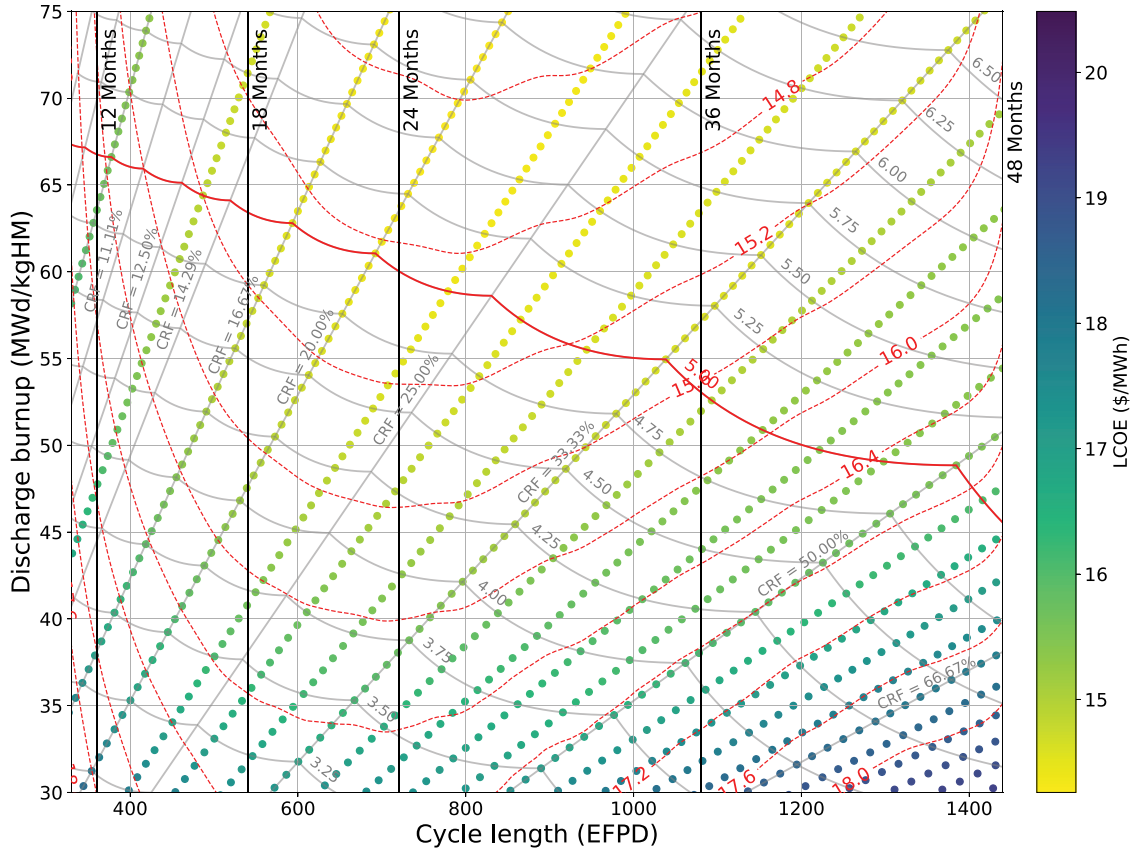

Fig. 4. Economic performance trends under the favorable input assumptions shown for varying cycle lengths and CRFs, assuming outage duration is independent of cycle length. The red dashed lines indicate isometric contour levels of constant LCOE. Minor artifacts are visible caused by interpolation in regions with uneven data point density.

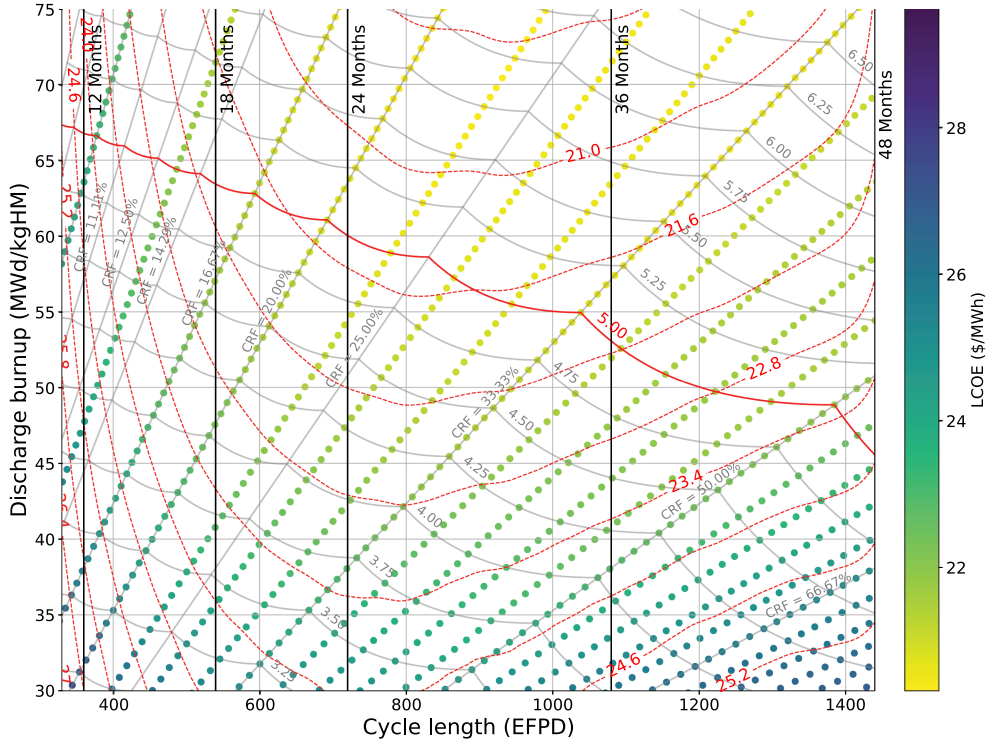

Fig. 5. Economic performance trends in the baseline scenario, where either the most probable value for triangular distributions or the mean value for uniform distributions was adopted. The results are shown for varying cycle lengths and CRFs, assuming outage duration is independent of cycle length. Minor artifacts are visible caused by interpolation in regions with uneven data point density.

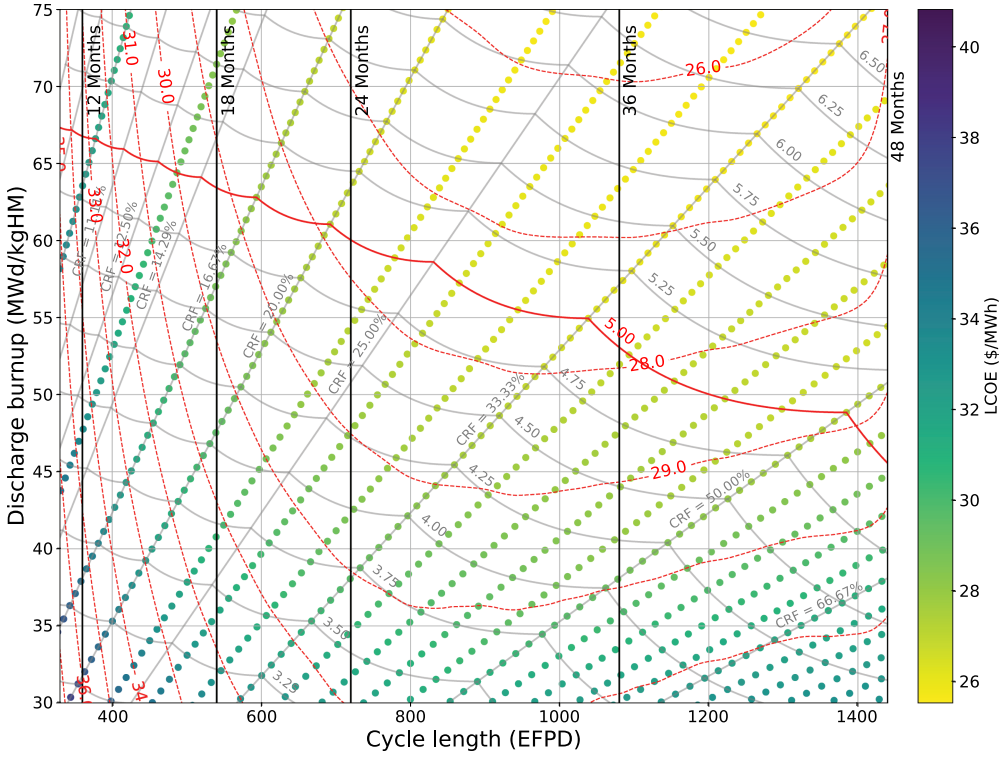

Fig. 6. Economic performance trends under the unfavorable input assumptions shown for varying cycle lengths and CRFs, assuming outage duration is independent of cycle length. The red dashed lines indicate isometric contour levels. Minor artifacts are visible caused by interpolation in regions with uneven data point density.

high-burnup fuel would be instrumental for these benefits to materialize.

2. Gradients become steeper far from the optimum and progressively smoother near it. Cycle lengths between 24 months and 36 months offer solutions relatively insensitive to economic outlook variations.

These considerations do not apply under baseline conditions with extended outages beyond 24-month cycles (Fig. 7), where an additional 10 outage days were assumed for mid-cycle inspections. In this scenario, increasing the cycle length beyond 24 months, whether by raising CRF or batch enrichment, does not provide economic benefit.

In markets prioritizing sustainability over economic performance, adopting shorter cycle lengths provides substantial benefits in fuel utilization, as illustrated in Fig. 8. For instance, considering an average discharge burnup of 50 MWd/kg HM, 12-month cycles exhibited an improvement in fuel utilization of approximately 20% compared to 36-month cycles, albeit with a trade-off in economic performance and outage schedule.

By overlapping sustainability and economic performance trends, 24-month cycles emerged as the most balanced option, offering a favorable compromise between LCOE and fuel utilization. Compared to shorter cycles, 24-month cycles demonstrated improved economic performance with reduced sensitivity to economic outlook. Conversely, when compared to longer cycles, they provided improvements in fuel utilization while retaining similar or better economic performance, particularly within the current regulatory framework governing maintenance frequency.

Before presenting the sensitivity analysis results, it is essential to address the technical constraints that may limit the arbitrary selection of cycle length or CRF. These constraints arise from fundamental design and safety considerations, which must be satisfied to ensure compliance with licensing requirements and operational reliability.

The first limiting factor concerns the average discharge burnup. The selected FA design is licensed for a maximum pin-averaged burnup of 62 MWd/kg HM, with potential extension up to 68 MWd/kg HM for

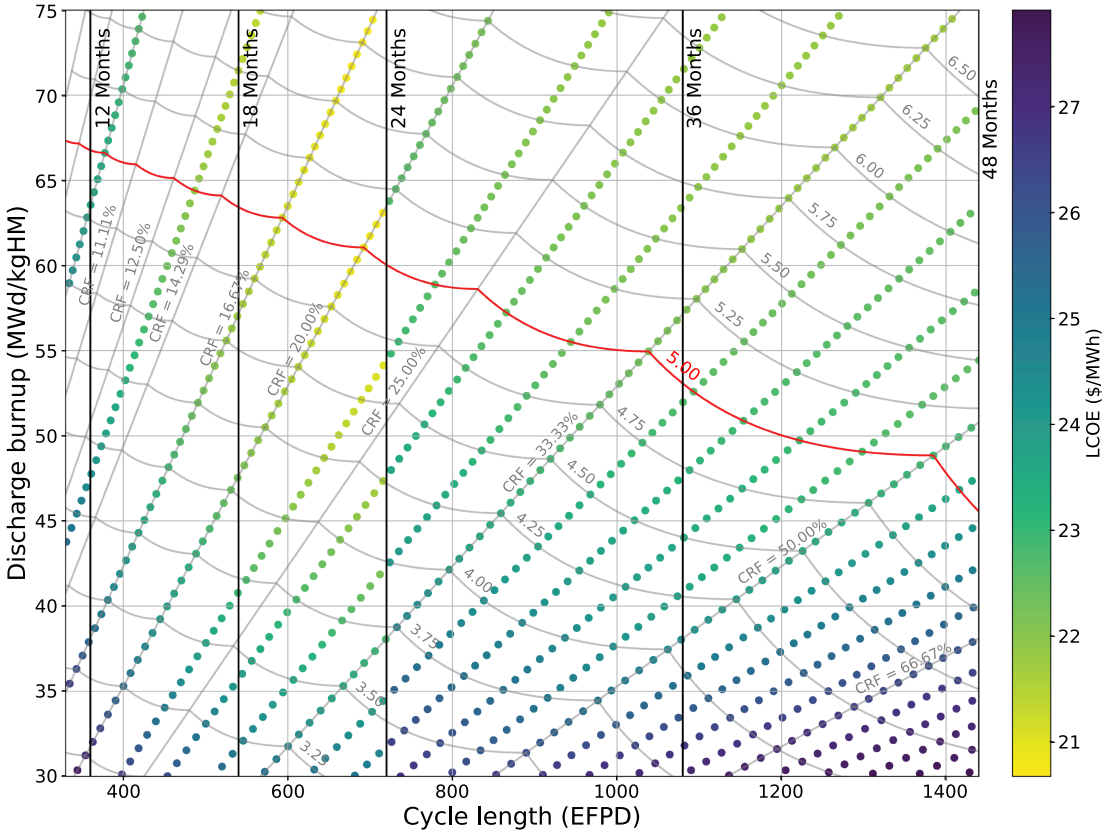

Fig. 7. Economic performance trends adopting baseline economic input data, retaining current LWR regulations on maintenance frequency.

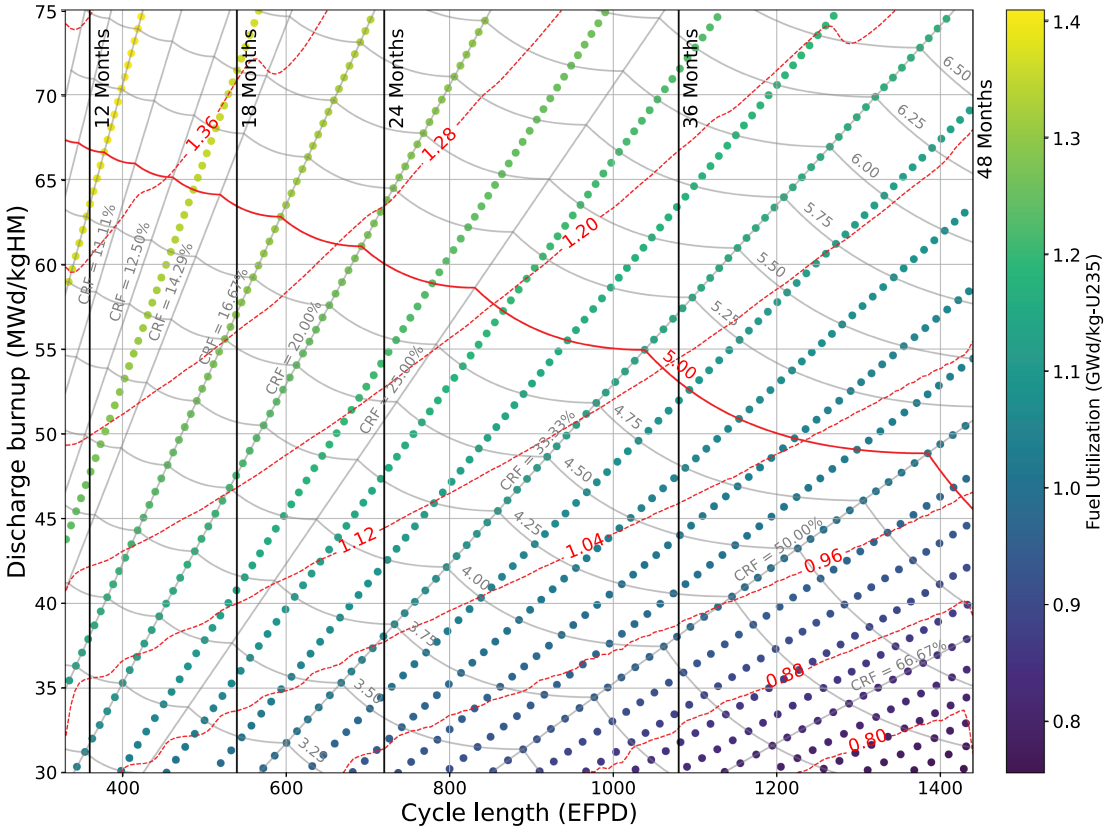

Fig. 8. Fuel utilization trends of the SMR under study for different cycle lengths and CRFs. The red dashed lines represent isometric contours of equal fuel utilization, illustrating the spatial distribution and boundaries of regions with identical values.

assemblies located at the core periphery, where the power densities are significantly lower.

In the hypothesis of constant power density, we can only determine the average FA discharge burnup, neglecting effects related to core leakages and intra-assembly gradients, which alter local burnup distributions. Selecting a configuration with an average discharge burnup excessively close to the pin burnup limit, a detailed power reconstruction might conclude that the selected cycle length and/or CRF does not guarantee the required safety margins.

The second limiting factor is related to the in-core fuel residence time, expressed as $\lceil N \rceil T_c$. At reduced power densities, the time required to accrue discharge burnup levels typical of large commercial PWRs increases substantially. For instance, achieving a discharge burnup of 50 MWd/kg HM implies a fuel residence time of 9 years for 18-month and 36-month cycles, and up to 10 years for a fraction of the core in 24-month cycles.

These in-core residence times are beyond current operational experience for current PWR FA designs; therefore, suitable measures may need to be adopted to ensure compliance with creep, crud deposition, and fuel bow design criteria, for example. For instance, a judicious choice of CRF for the initial cycles allows for keeping the residence time within the current operational envelope, followed by the gradual transition to smaller CRF with longer residence times as experience basis is gained.

The third limiting factor relates to refueling operations. During refueling, FAs are temporarily transferred to the spent fuel pool before being reshuffled inside the core. Adopting smaller CRF values could increase the likelihood of fuel handling–related damages, as the total number of assembly displacements grows inversely with CRF.

In this context, extending the cycle length offers a dual advantage, in that it decreases the total number of refueling campaigns over the plant lifetime and reduces the cumulative amount of fuel transitioned into the spent fuel pool. Both effects contribute to lowering operational exposure and mitigating risks associated with fuel handling activities.

Finally, all configurations must maintain adequate safety margins to prevent fuel damage during anticipated operational occurrences and design-basis accidents, and to

mitigate the consequences of beyond design-basis accidents. These requirements impose strict limits on thermal-hydraulic behavior, reactivity control, and mechanical integrity throughout the extended fuel residence time.

III.B. Sensitivity Studies and Cost Breakdown

This section presents the local and global sensitivity studies, with results grouped by equivalent cycle length to examine the effect of CRF. For each cycle length, a reference scenario was selected to normalize the LCOE distribution, enabling a consistent comparison of economic performance under equivalent cost conditions. Reference configurations were chosen to achieve an average discharge burnup of approximately 50 MWd/kg HM, a target routinely met by large PWRs. This target also provides adequate margins for compliance with design criteria on maximum averaged rod burnup, although apropriate measures to ensure fuel integrity for extended residence times may still be required for some scenarios.

III.B.1. 12-Month Cycles

Cycles of 12 months offer improved fuel utilization at the expense of reduced plant availability and economic performance, providing attractive solutions for markets favoring shorter cycle lengths, such as Japan. The economic and sustainability performance for 12-month cycles, illustrated in Fig. 9, reports, for each CRF, the predicted enrichment, average discharge

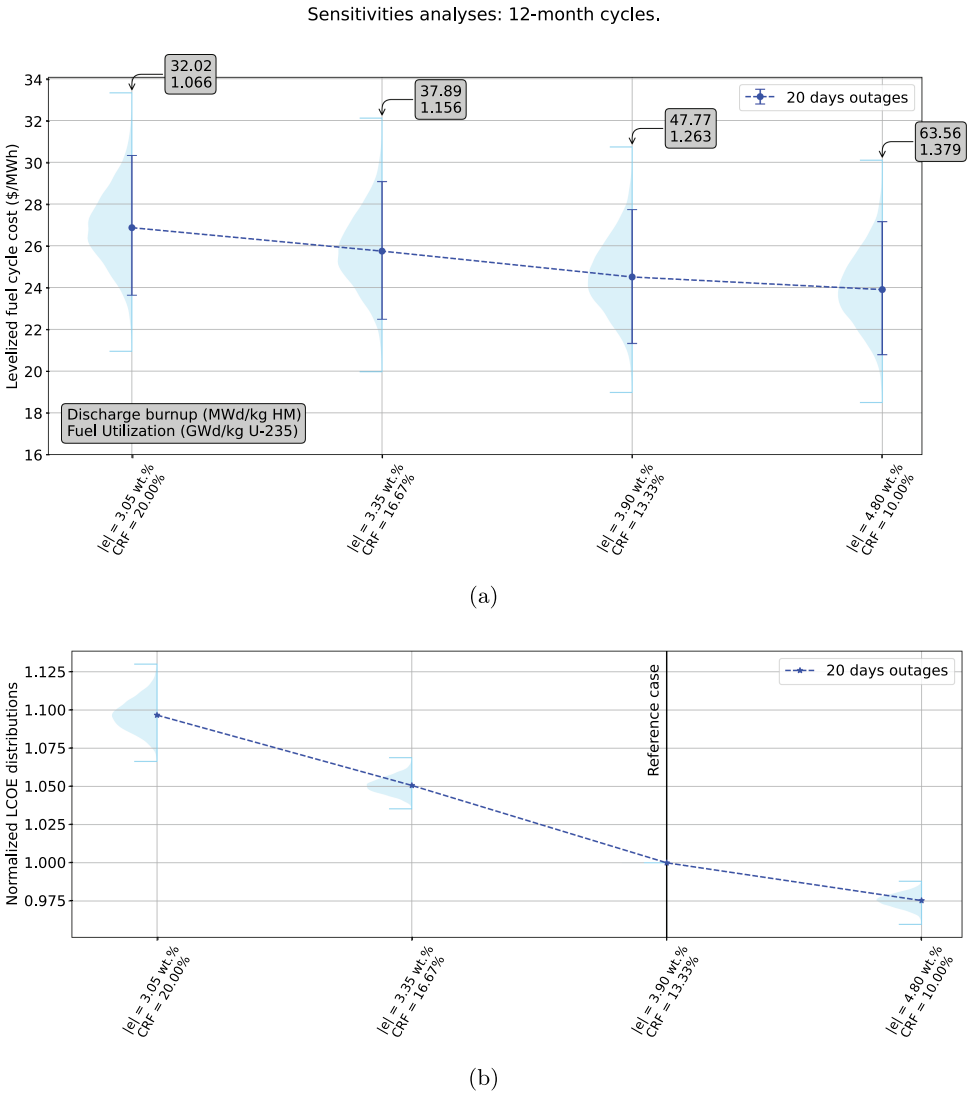

Fig. 9. Global sensitivity analysis results for 12-month cycles: (a) shows for each CRF, the predicted enrichment, fuel utilization, and average discharge burnup alongside the LCOE distribution (light blue) and its central 95% quantile interval (dark blue), and (b) presents the normalized LCOE distributions, enabling a comparison under equivalent cost scenarios.

burnup, and fuel utilization. In addition, the LCOE distributions, obtained by independently sampling the economic input parameters 10 000 times, are presented.

Normalized distributions are also shown, considering a reference scenario characterized by a 13.33%*CRF* and an average discharge burnup of approximately 47 MWd/kg HM, corresponding to a maximum fuel residence time of 8 years. These normalized distributions indicate that the reference configuration achieved improved economic performance compared to larger CRF values. Further reductions in CRF could enhance economic performance and fuel utilization; however, technical limitations on maximum pin discharge burnup leave minimal margins for core optimization.

The results of the local sensitivity analysis are summarized in Table 8, which reports the marginal impact of a 10% increase in each cost component. Among these, C_{ore} and C_{SWU} emerge as the dominant drivers, as a 10% increase in their respective prices leads to approximately 2.5% and 2.0% increases in LCOE. Outage-related expenses also remain significant, as a 10% increase in either average salaries or working hours translates into roughly a 2% rise in the total costs. Finally, replacement energy costs rank fourth in importance, with their marginal impact amounting to about two-thirds of that associated with worker-related expenses.

These findings are confirmed by the cost breakdowns shown in Fig. 10. In particular, outage costs dominate in 12-month cycles because of a lower plant availability. As CRF increases (and fissile utilization decreases), ore-related and enrichment costs rise, typically representing the second and third most significant contributors. Conversely, the contribution of in-core carrying charges grows as CRF decreases, reflecting the longer fuel residence time.

III.B.2. 18-Month Cycles

Cycles of 18 months exhibit improved overall economic performance compared to 12-month cycles, albeit with a modest reduction in fuel utilization. The results of the global sensitivity analysis are shown in Fig. 11. The reference configuration, characterized by a 20.0%*CRF*, reduces the fuel residence time to approximately 7.5 years and improves the economic performance by about 6%, while only marginally decreasing fuel utilization ($\approx 4\%$) relative to 12-month cycles.

For higher CRF values, the considerations discussed for 12-month cycles remain applicable to 18-month cycles. Conversely, a 16.67%*CRF* offers greater flexibility for local burnup optimization, with potential gains in both economic performance and fuel utilization, though at the cost of extending fuel residence time to nearly 9 years.

Local sensitivity results, presented in Table 9, indicate that a 10% increase in ore-related costs and enrichment costs led to approximately 3% and 2.5% increases in LCOE, respectively. Improved plant availability mitigatec the impact of labor-related expenses, with a 10% increase in salaries or working hours resulting in only about a 1.5% rise in the total costs. Furthermore, the impact of replacement energy costs observed for 12-month cycles extended to 18-month cycles; however, at higher CRF values, fabrication costs become the fourth most significant contributor.

The cost breakdown in Fig. 12 confirms the dominant role of outage-related expenses, particularly at lower CRF values. Ore-related costs represent the second most significant contributor, closely followed by enrichment-related expenses, and especially at lower CRF values, operational carrying charges.

TABLE 8

Marginal Impact on LCOE ($/MWh) of a 10% Increase in Individual Cost Components for 12-Month Cycles with the Results Grouped by Cost Category: Fuel-Related, Spent Fuel, and Outage-Related Expenses

Marginal Impact on LCOE of a 10% Increase in Individual Cost Components ($/MWh)									
Fuel Related					Spent Fuel			Outages	
CRF (%)	C_{ore}	C_{conv}	C_{SWU}	C_{fabr}	$C_{tax,ele}$	$C_{tax,mass}$	$C_{tax,\mathrm{FA}}$	$C_{\mathrm{labor}}/h_{\mathrm{labor}}$	$C_{\mathrm{ele,r}}$
10.00	0.615	0.145	0.520	0.157	0.044	0.066	0.007	0.486	0.333
13.34[(ref)]	0.618	0.146	0.491	0.193	0.052	0.104	0.011	0.485	0.333
16.67	0.638	0.150	0.480	0.232	0.061	0.154	0.017	0.489	0.335
20.00	0.667	0.157	0.483	0.266	0.066	0.197	0.021	0.482	0.331

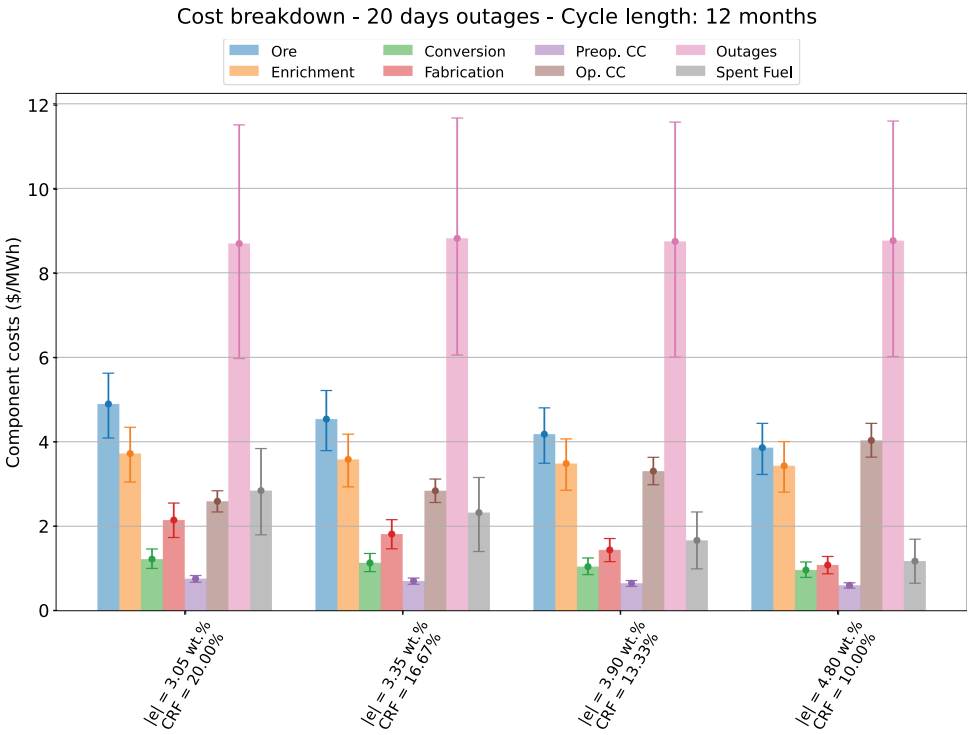

Fig. 10. Cost breakdown for 12-month cycles. For each CRF, the predicted enrichment and the contribution of individual cost components are shown. Shaded bars represent the central 95% quantile interval for each component.

TABLE 9

Marginal Impact on LCOE ($/MWh) of a 10% Increase in Individual Cost Components for 18-Month Cycles with the Results Grouped by Cost Category: Fuel-Related, Spent Fuel, and Outage-Related Expenses

Marginal Impact on LCOE of a 10% Increase in Individual Cost Components ($/MWh)									
Fuel Related					Spent Fuel			Outages	
CRF (%)	C_{ore}	C_{conv}	C_{SWU}	C_{fabr}	$C_{tax,ele}$	$C_{tax,mass}$	$C_{tax,\mathrm{FA}}$	$C_{\mathrm{labor}}/h_{\mathrm{labor}}$	$C_{\mathrm{ele,r}}$
16.67	0.635	0.150	0.531	0.169	0.049	0.081	0.009	0.325	0.223
20.00[(ref)]	0.641	0.151	0.516	0.193	0.055	0.110	0.012	0.325	0.223
23.34	0.662	0.156	0.516	0.218	0.055	0.128	0.014	0.325	0.223
26.67	0.683	0.161	0.520	0.241	0.062	0.163	0.018	0.321	0.220
30.00	0.709	0.167	0.527	0.265	0.062	0.182	0.020	0.321	0.220

III.B.3. 24-Month Cycles

Cycles of 24 months represent the state of the art for existing large PWR technology and have driven efforts to extend enrichment regulatory limits beyond 5.0 wt%, for what concerns high power density plants.

The results for 24-month cycles are presented in Fig. 13. Compared to 18-month cycles, this configuration offers further improvements in economic performance, primarily originated by enhanced plant availability. As anticipated in the previous section, a minimum in LCOE was observed for CRF values between 20% and 25%. The selected reference configuration, characterized by a 26.67% CRF, improved economic performance by approximately 5% in comparison to the reference case for an 18-month cycle, with the trade-off of a minor reduction in fuel utilization ($\approx$ 5%) and a fuel residence time of 8 years.

Economic performance and fuel utilization can be further improved by adopting a 23.34% CRF, at the cost

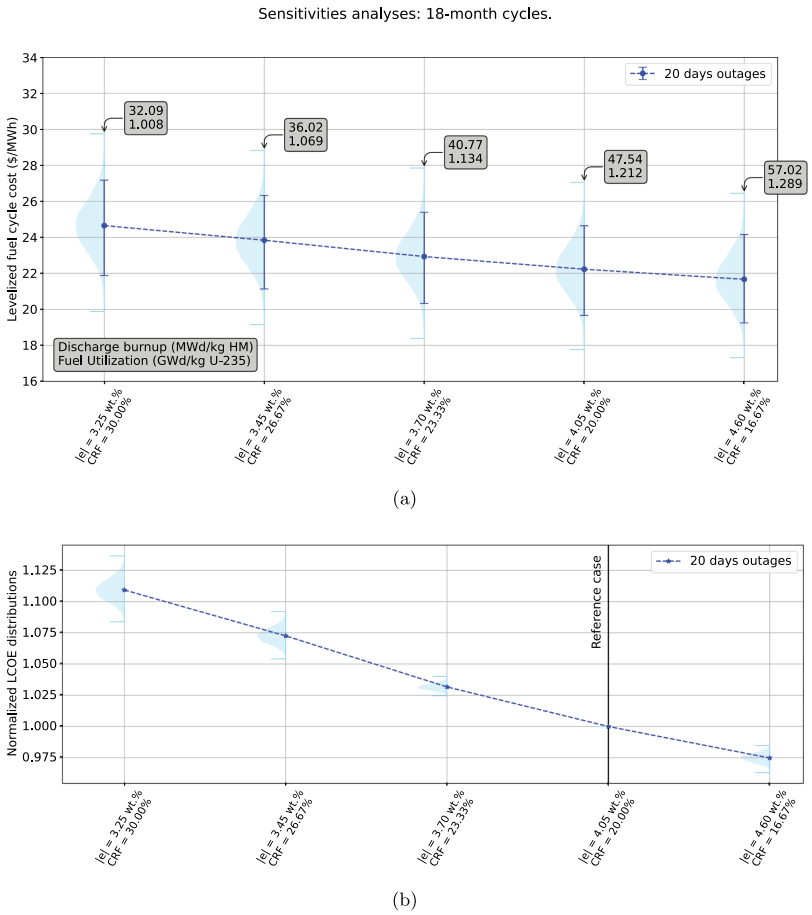

Fig. 11. Global sensitivity analysis results for 18-month cycles: (a) shows, for each CRF, the predicted enrichment, fuel utilization, and average discharge burnup alongside the LCOE distribution (light blue) and its central 95% quantile interval (dark blue) and (b) presents the normalized LCOE distributions, enabling a comparison under equivalent cost scenarios.

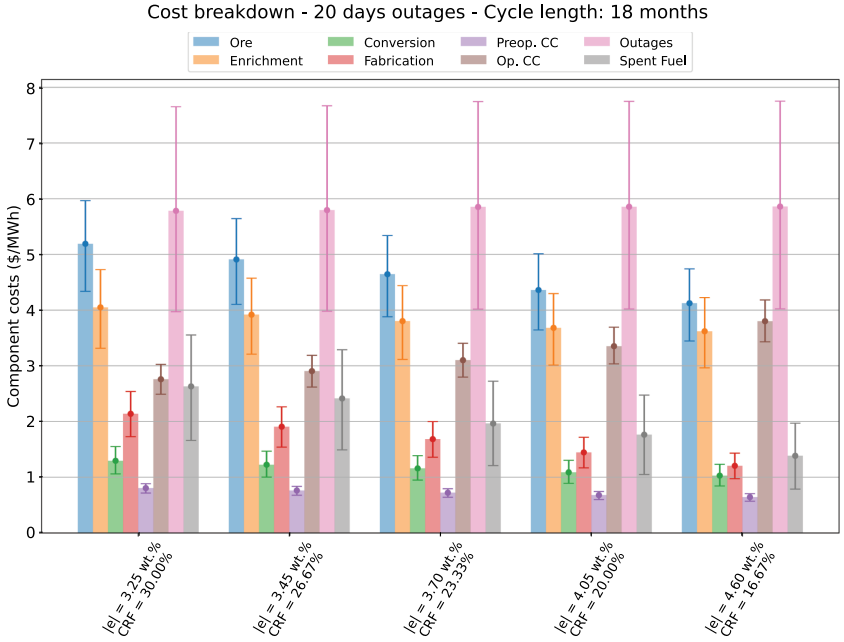

Fig. 12. Cost breakdown for 18-month cycles. For each CRF, the predicted enrichment and the contribution of individual cost components are shown. Shaded bars represent the central 95% quantile interval for each component.

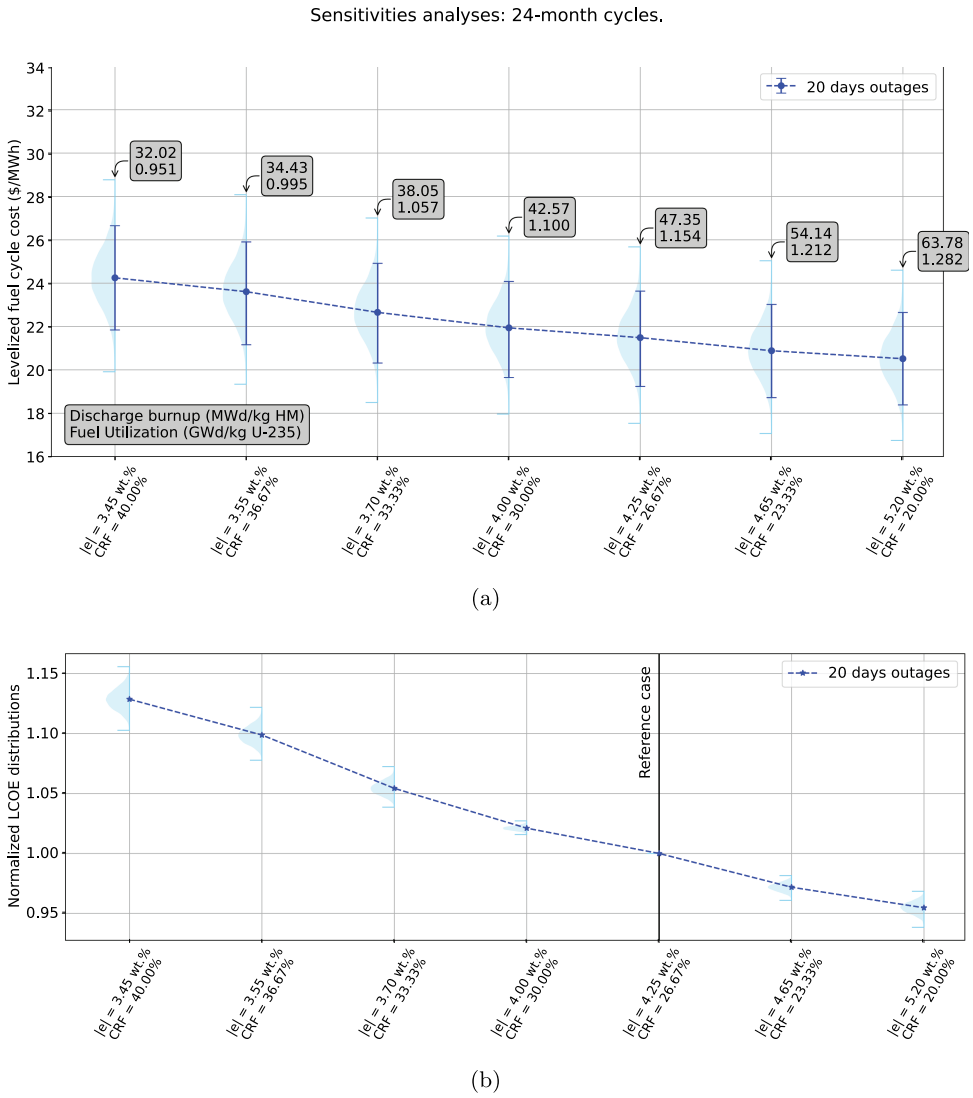

Fig. 13. Global sensitivity analysis results for 24-month cycles: (a) shows, for each CRF, the predicted enrichment, fuel utilization, and average discharge burnup alongside the LCOE distribution (light blue) and its central 95% quantile interval (dark blue), and (b) presents the normalized LCOE distributions, enabling a comparison under equivalent cost scenarios.

of increasing the fuel residence time to 10 years and reducing the pin burnup margins. Additional reductions in CRF would continue to enhance economic performance without altering the fuel residence time, but at the expense of further reducing the pin burnup margins and requiring LEU+ fuel.

Local sensitivity results, reported in Table 10, revealed a similar outlook to 18-month cycles, with comparable effects from marginal increases in C_{ore} and C_{SWU}. Improved plant availability further reduces the contribution of outage-related expenses, which still represent the third and fourth contributors at lower CRF values, albeit with reduced magnitude. At higher CRF values, fabrication costs become the third most significant contributor, while fees associated with spent fuel mass surpass replacement energy costs in importance.

The cost breakdown analysis in Fig. 14 confirms that ore-related costs consistently dominated the overall cost structure at higher CRF values. At lower CRF values, the relative importance of outage-related expenses and operational carrying charges becomes comparable to ore-related costs. In particular, for operational carrying charges, the observations reinforced the trend that longer cycle lengths and higher discharge burnup, implying extended fuel residence times, make operational carrying charges a major cost component.

TABLE 10

Marginal Impact on LCOE ($/MWh) of a 10% Increase in Individual Cost Components for 24-Month Cycles with the Results Grouped by Cost Category: Fuel-Related, Spent Fuel, and Outage-Related Expenses

Marginal Impact on LCOE of a 10% Increase in Individual Cost Components ($/MWh)									
Fuel Related					Spent Fuel			Outages	
CRF (%)	C_{ore}	C_{conv}	C_{SWU}	C_{fabr}	$C_{tax,ele}$	$C_{tax,mass}$	$C_{tax,\mathrm{FA}}$	$C_{\mathrm{labor}}/h_{\mathrm{labor}}$	$C_{\mathrm{ele,r}}$
20.00	0.659	0.155	0.570	0.155	0.045	0.067	0.007	0.242	0.166
23.34	0.666	0.157	0.559	0.175	0.045	0.080	0.009	0.244	0.168
26.67[(ref)]	0.675	0.159	0.551	0.194	0.053	0.107	0.012	0.245	0.168
30.00	0.691	0.163	0.554	0.211	0.053	0.118	0.013	0.242	0.166
33.34	0.698	0.164	0.544	0.230	0.062	0.155	0.017	0.243	0.167
36.67	0.730	0.172	0.561	0.250	0.062	0.172	0.019	0.245	0.168
40.00	0.754	0.178	0.573	0.266	0.062	0.184	0.020	0.241	0.165

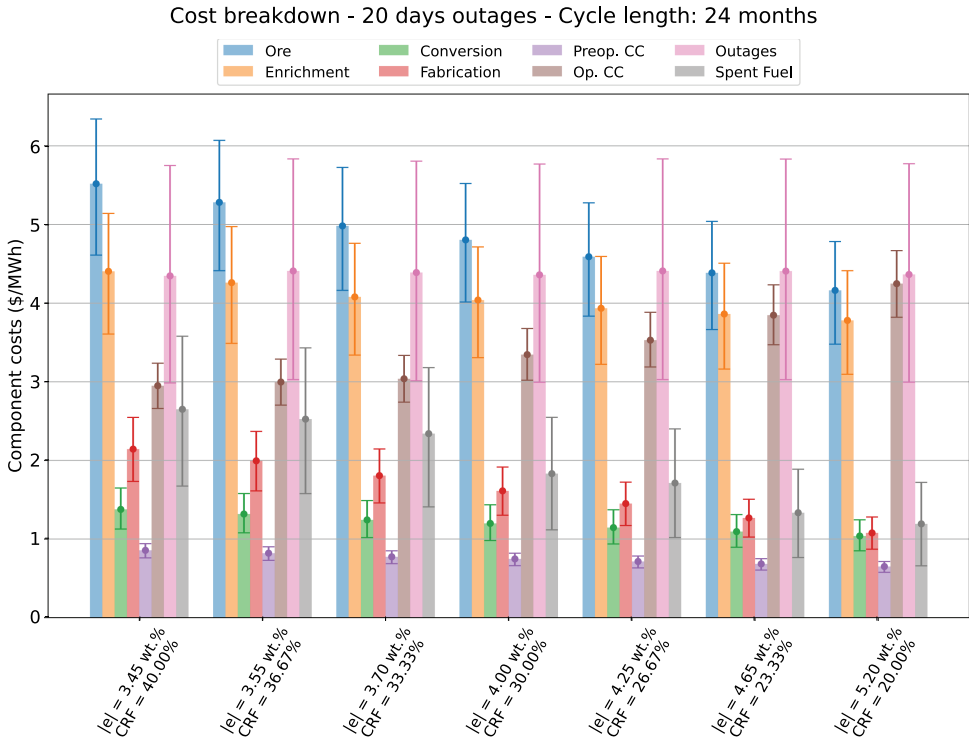

Fig. 14. Cost breakdown for 24-month cycles. For each CRF, the predicted enrichment and the contribution of individual cost components are shown. Shaded bars represent the central 95% quantile interval for each component.

III.B.4. 36-Month Cycles

Cycles of 36 months represent an innovative fuel management strategy proposed for SMRs, favored in reduced power density designs.

The economic performance of 36-month cycles, illustrated in Fig. 15, is broadly comparable to that of 24-month cycles, though accompanied by a substantial reduction in fuel utilization balanced by the larger availability factor in terms of net economic performance. For example, at equal average discharge burnup (40.0%*CRF*), fuel utilization decreases by approximately 10%. To leverage improved pin burnup margins, a reference configuration with 36.67%*CRF* was selected, offering enhanced fuel utilization and economic

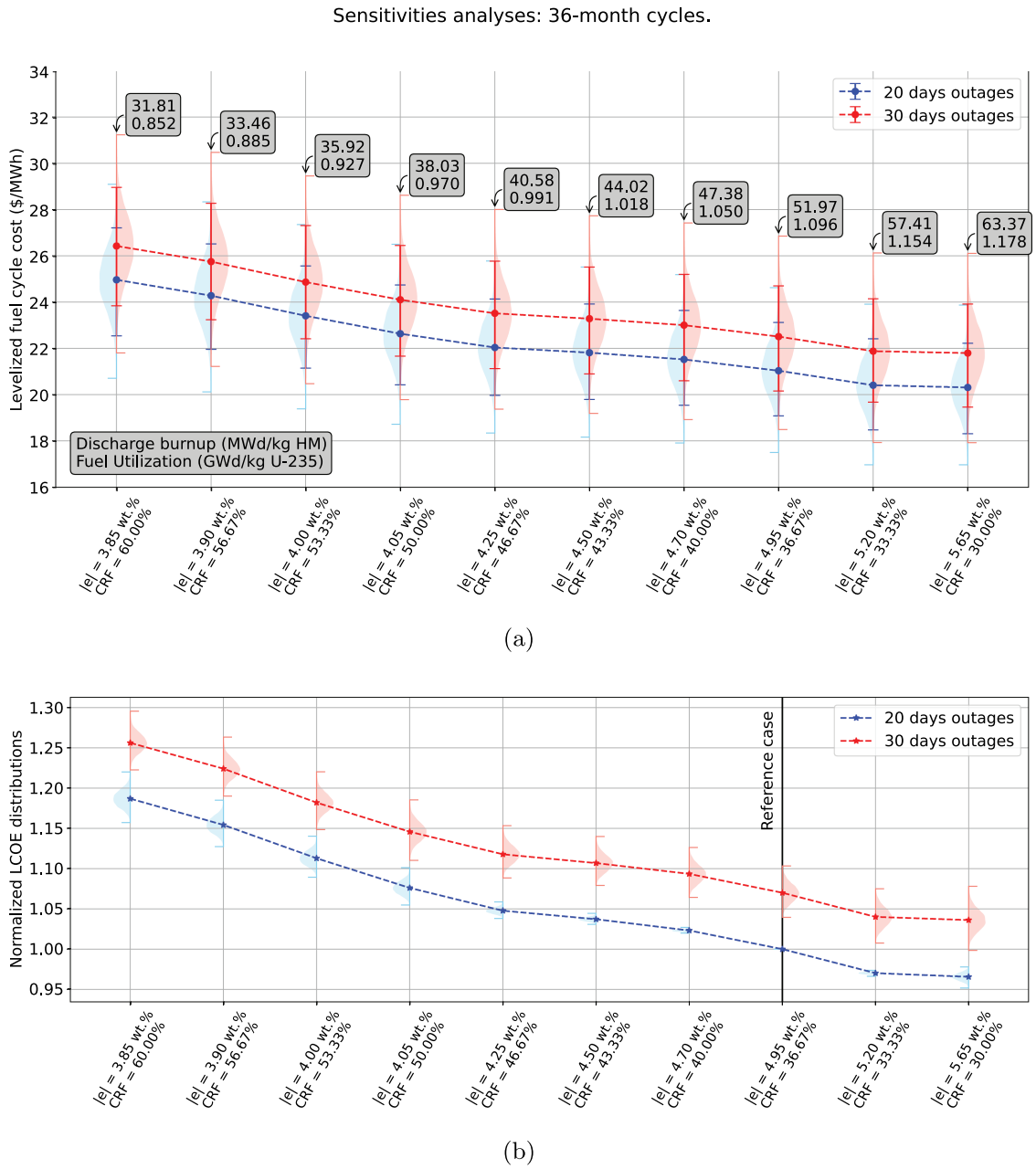

Fig. 15. Global sensitivity analysis results for 36-month cycles: (a) shows, for each CRF, the predicted enrichment, fuel utilization, and average discharge burnup, along with the LCOE distribution (light blue for 20 outage days) and its central 95% quantile interval (dark blue), and (b) presents the normalized LCOE distributions for a comparison under equivalent cost scenarios. Additionally, the LCOE distributions for extended outages (pink) and their 95% quantile intervals (red) are also reported.

performance at the cost of operating near current enrichment regulatory limits.

Further reductions in CRF values could yield additional economic benefits while preserving pin burnup margins, but would require LEU+ fuel.

Beyond this point, additional reductions in CRF provide negligible economic advantages, aside from minor improvements in fuel utilization caused by a sharp increase in operational carrying charges associated with fuel residence times approaching 12 years. In the extended outage scenario, economic performance would deteriorate by approximately 1.5 $/MWh, as shown in Fig. 16.

Local sensitivity analyses, reported in Tables 11 and 12, revealed trends similar to those observed for 24-month cycles. At lower CRF values, fabrication and conversion costs exhibited an influence comparable to labor-related

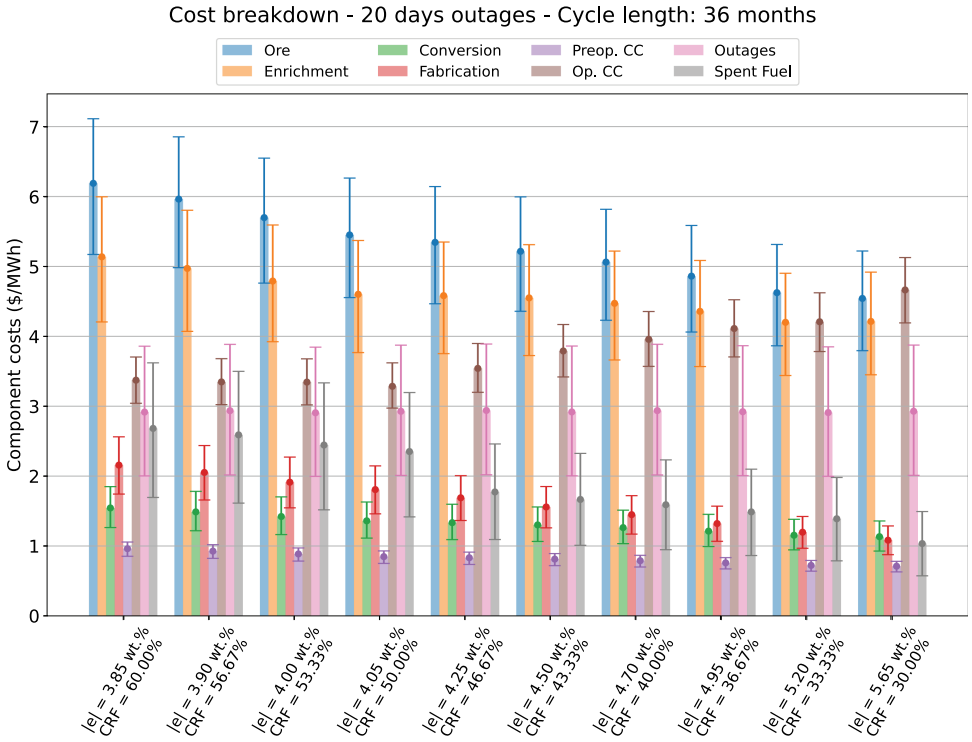

(a)

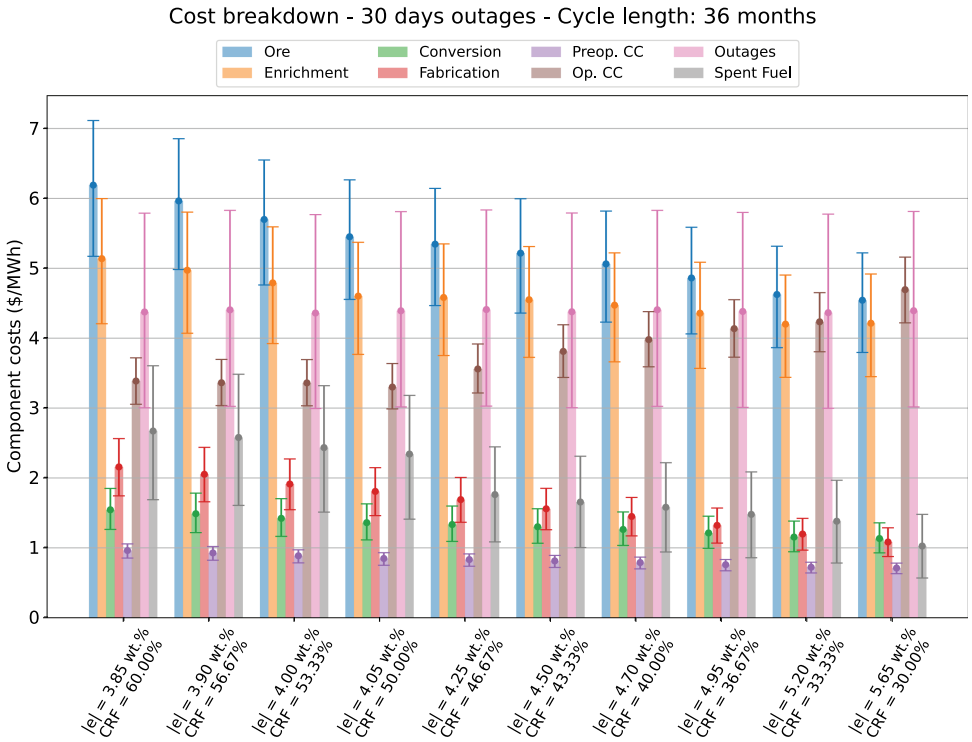

(b)

Fig. 16. Cost breakdown for 36-month cycles. For each CRF, the predicted enrichment and the contribution of individual cost components are shown, with shaded bars representing the central 95% quantile interval. (a) Illustrates the cost breakdown assuming 20 outage days, while (b) reports the results for extended outage conditions.

expenses, while at higher CRF values they become the third and fourth most significant contributors, respectively. Under extended outage conditions, outage-related expenses regained their role as the third and fourth contributors.

III.B.5. 48-Month Cycles

Cycles of 48 months have been considered as an advanced fuel management strategy for SMRs. In this work, we assessed their economic performance, acknowledging that technical challenges (not discussed here) may ultimately constrain the feasibility space of core design options supporting such extended cycles. The results, presented in Fig. 17, indicate consistently similar economic performance compared to shorter cycle lengths. In this context, the role of LEU+ fuel becomes essential to achieve the target discharge burnup of 50 MWd/kg HM. Further reductions in CRF below the 50% threshold yielded only marginal improvements in the economic and sustainability metrics, while increasing fuel residence time to approximately 12 years.

TABLE 11

Marginal Impact on LCOE ($/MWh) of a 10% Increase in Individual Cost Components for 36-Month Cycles, Considering 20 Days of Outages, with the Results Grouped by Cost Category: Fuel-Related, Spent Fuel, and Outage-Related Expenses

Marginal Impact on LCOE of a 10% Increase in Individual Cost Components ($/MWh)									
Fuel Related					Spent Fuel			Outages	
CRF (%)	C_{ore}	C_{conv}	C_{SWU}	C_{fabr}	$C_{tax,ele}$	$C_{tax,mass}$	$C_{tax,\mathrm{FA}}$	$C_{\mathrm{labor}}/h_{\mathrm{labor}}$	$C_{\mathrm{ele,r}}$
30.00	0.720	0.170	0.636	0.156	0.039	0.058	0.006	0.162	0.111
33.34	0.709	0.167	0.614	0.167	0.049	0.081	0.009	0.161	0.111
36.67(ref)	0.732	0.173	0.625	0.181	0.049	0.090	0.010	0.162	0.111
40.00	0.748	0.176	0.629	0.194	0.049	0.099	0.011	0.163	0.112
43.34	0.758	0.179	0.630	0.206	0.049	0.106	0.011	0.162	0.111
46.67	0.761	0.179	0.622	0.219	0.049	0.116	0.012	0.163	0.112
50.00	0.762	0.180	0.613	0.230	0.062	0.156	0.017	0.162	0.111
53.34	0.793	0.187	0.635	0.242	0.062	0.165	0.018	0.161	0.111
56.67	0.823	0.194	0.653	0.257	0.063	0.178	0.019	0.163	0.112
60.00	0.849	0.200	0.671	0.269	0.062	0.186	0.020	0.162	0.111

TABLE 12

Marginal Impact on LCOE ($/MWh) of a 10% Increase in Individual Cost Components for 36-Month Cycles, Considering 30 Days of Outages, with the Results Grouped by Cost Category: Fuel-Related, Spent Fuel, and Outage-Related Expenses

Marginal Impact on LCOE of a 10% Increase in Individual Cost Components ($/MWh)									
Fuel Related					Spent Fuel			Outages	
CRF (%)	C_{ore}	C_{conv}	C_{SWU}	C_{fabr}	$C_{tax,ele}$	$C_{tax,mass}$	$C_{tax,\mathrm{FA}}$	$C_{\mathrm{labor}}/h_{\mathrm{labor}}$	$C_{\mathrm{ele,r}}$
30.00	0.722	0.170	0.637	0.156	0.039	0.058	0.006	0.244	0.167
33.34	0.711	0.168	0.615	0.167	0.049	0.081	0.009	0.242	0.166
36.67(ref)	0.733	0.173	0.626	0.181	0.049	0.090	0.010	0.243	0.167
40.00	0.749	0.177	0.630	0.195	0.049	0.099	0.011	0.244	0.168
43.33	0.759	0.179	0.630	0.206	0.049	0.106	0.011	0.243	0.166
46.67	0.762	0.180	0.622	0.219	0.049	0.115	0.012	0.245	0.168
50.00	0.763	0.180	0.613	0.230	0.062	0.156	0.017	0.244	0.167
53.33	0.793	0.187	0.635	0.242	0.062	0.164	0.018	0.242	0.166
56.67	0.823	0.194	0.654	0.257	0.062	0.177	0.019	0.244	0.167
60.00	0.850	0.200	0.672	0.269	0.062	0.185	0.020	0.243	0.166

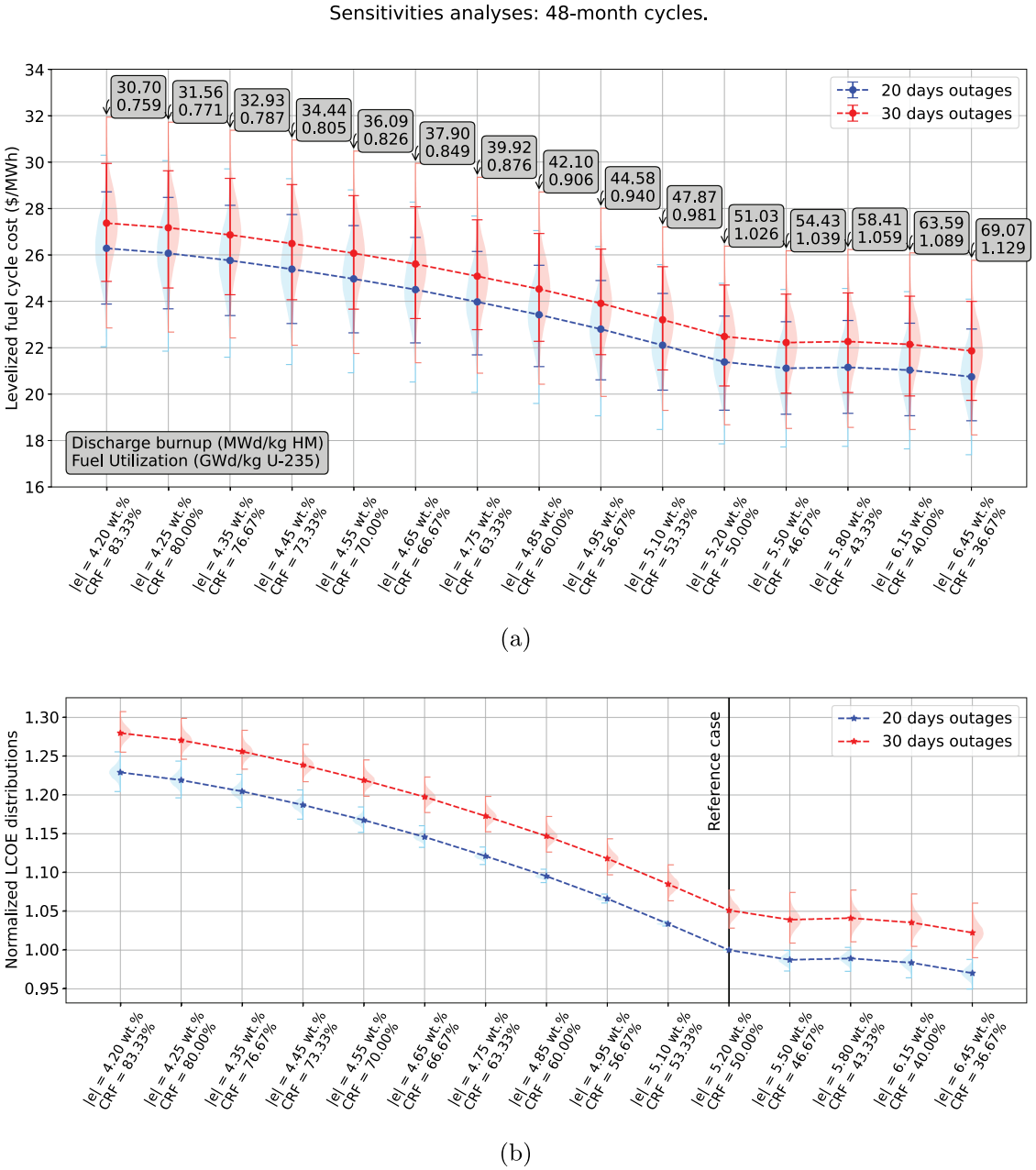

Fig. 17. Global sensitivity analysis results for 48-month cycles: (a) shows, for each CRF, the predicted enrichment, fuel utilization, and average discharge burnup, along with the LCOE distribution (light blue for 20 outage days) and its central 95% quantile interval (dark blue), and (b) presents the normalized LCOE distributions for a comparison under equivalent cost scenarios. Additionally, LCOE distributions for extended outages (pink) and their 95% quantile intervals (red) are also reported.

Regarding outage extensions, the trends observed for 36-month cycles remained valid, with an overall increase in LCOE of about 1.0 $/MWh, primarily absorbed by outage-related costs, as illustrated in Fig. 18. Local sensitivity analyses, reported in Tables 13 and 14, confirm conclusions drawn for 36-month cycles, although conversion and fabrication costs remained the dominant third and fourth contributors even at lower CRF values. In this context extended outages and labor-related costs have similar effects compared to conversion costs.

IV. CONCLUSION

In this work, we characterized trends in economic performance for a 300-MW(electric) SMR of a PWR type for different cycle lengths and CRF values. This analysis

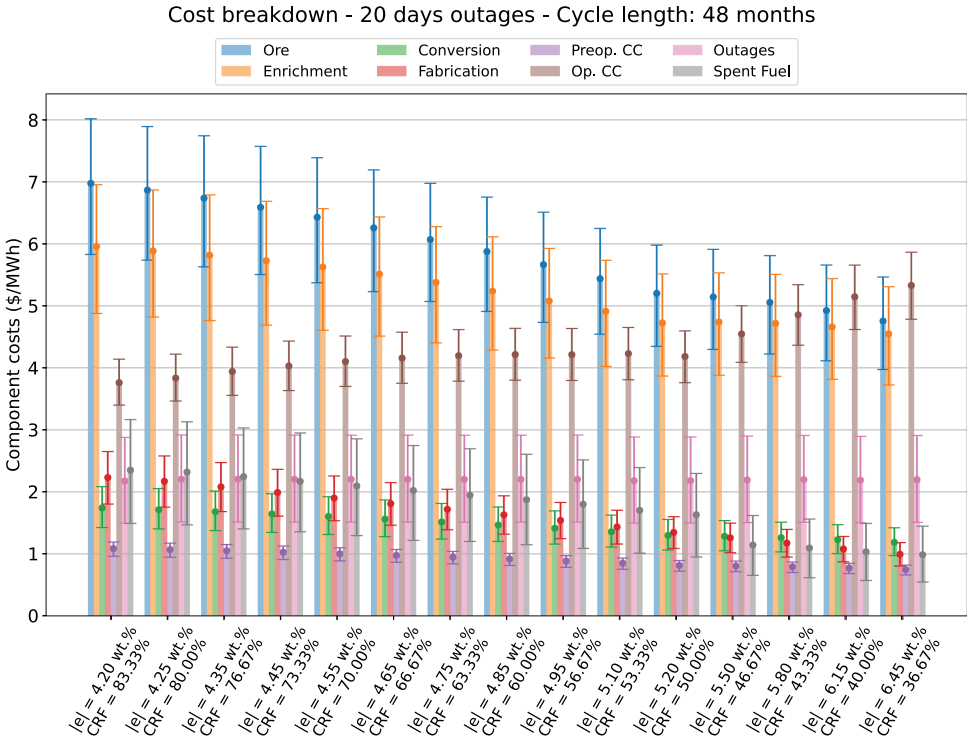

(a)

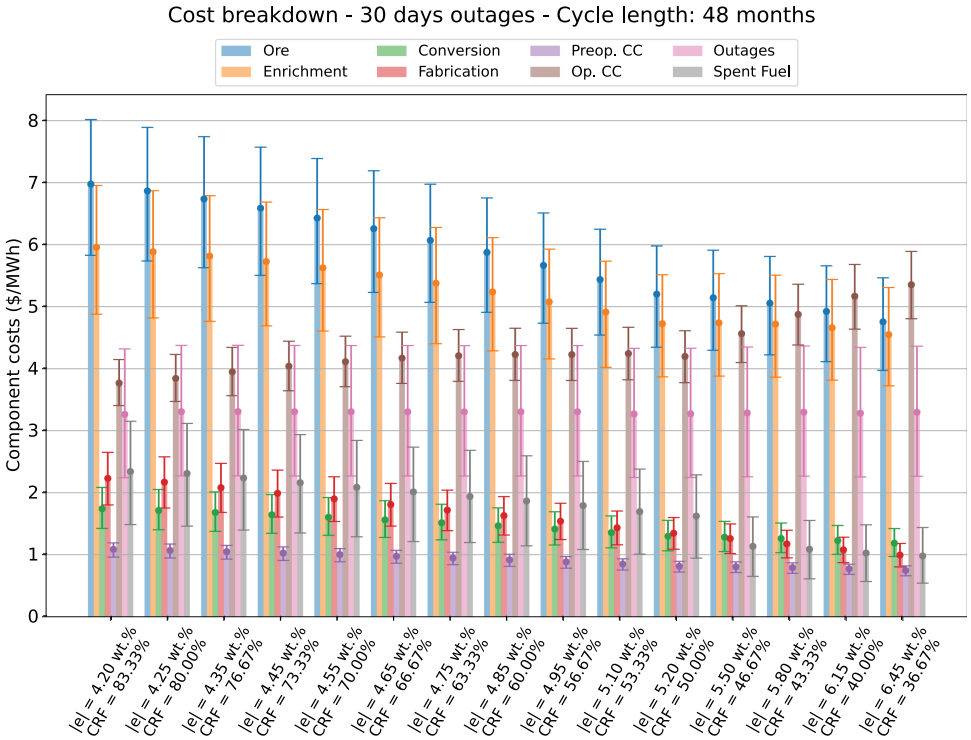

(b)

Fig. 18. Cost breakdown for 48-month cycles. For each CRF, the predicted enrichment and the contribution of individual cost components are shown, with shaded bars representing the central 95% quantile interval. (a) Illustrates the cost breakdown assuming 20 outage days, while (b) reports the results for extended outage conditions.

TABLE 13

Marginal Impact on LCOE ($/MWh) of a 10% Increase in Individual Cost Components for 48-Month Cycles, Considering 20 Days of Outages, with the Results Grouped by Cost Category: Fuel-Related, Spent Fuel, and Outage-Related Expenses

Marginal Impact on LCOE of a 10% Increase in Individual Cost Components ($/MWh)									
Fuel Related					Spent Fuel			Outages	
CRF (%)	C_{ore}	C_{conv}	C_{SWU}	C_{fabr}	$C_{tax,ele}$	$C_{tax,mass}$	$C_{tax,\mathrm{FA}}$	$C_{\mathrm{labor}}/h_{\mathrm{labor}}$	$C_{\mathrm{ele,r}}$
36.67	0.774	0.182	0.705	0.147	0.039	0.054	0.006	0.122	0.084
40.00	0.785	0.185	0.707	0.156	0.039	0.058	0.006	0.121	0.083
43.34	0.787	0.186	0.700	0.166	0.039	0.064	0.007	0.122	0.084
46.67	0.783	0.185	0.687	0.174	0.039	0.068	0.007	0.122	0.083
50.00[(ref)]	0.774	0.182	0.669	0.182	0.053	0.099	0.011	0.121	0.083
53.34	0.802	0.189	0.691	0.192	0.053	0.106	0.011	0.121	0.083
56.67	0.828	0.195	0.707	0.204	0.054	0.114	0.012	0.122	0.084
60.00	0.851	0.201	0.723	0.215	0.054	0.121	0.013	0.122	0.084
63.34	0.873	0.206	0.736	0.225	0.054	0.128	0.014	0.122	0.084
66.67	0.892	0.210	0.748	0.234	0.054	0.134	0.014	0.122	0.084
70.00	0.909	0.214	0.758	0.244	0.054	0.141	0.015	0.122	0.084
73.34	0.924	0.218	0.765	0.254	0.054	0.148	0.016	0.122	0.084
76.67	0.937	0.221	0.770	0.263	0.054	0.155	0.017	0.122	0.084
80.00	0.947	0.223	0.773	0.272	0.054	0.161	0.017	0.122	0.084
83.34	0.956	0.225	0.778	0.278	0.053	0.164	0.018	0.121	0.083

TABLE 14

Marginal Impact on LCOE ($/MWh) of a 10% Increase in Individual Cost Components for 48-Month Cycles, Considering 30 Days of Outages, with the Results Grouped by Cost Category: Fuel-Related, Spent Fuel, and Outage-Related Expenses

Marginal Impact on LCOE of a 10% Increase in Individual Cost Components ($/MWh)									
Fuel Related					Spent Fuel			Outages	
CRF (%)	C_{ore}	C_{conv}	C_{SWU}	C_{fabr}	$C_{tax,ele}$	$C_{tax,mass}$	$C_{tax,\mathrm{FA}}$	$C_{\mathrm{labor}}/h_{\mathrm{labor}}$	$C_{\mathrm{ele,r}}$
36.67	0.775	0.183	0.706	0.147	0.039	0.054	0.006	0.183	0.125
40.00	0.786	0.185	0.708	0.157	0.039	0.058	0.006	0.182	0.125
43.34	0.788	0.186	0.700	0.166	0.039	0.063	0.007	0.183	0.125
46.67	0.784	0.185	0.688	0.174	0.039	0.068	0.007	0.182	0.125
50.00	0.774	0.183	0.670	0.182	0.053	0.099	0.011	0.182	0.124
53.34	0.803	0.189	0.691	0.193	0.053	0.105	0.011	0.181	0.124
56.67	0.828	0.195	0.707	0.205	0.053	0.114	0.012	0.183	0.126
60.00	0.852	0.201	0.723	0.215	0.053	0.121	0.013	0.183	0.126
63.34	0.873	0.206	0.737	0.225	0.053	0.127	0.014	0.183	0.126
66.67	0.893	0.210	0.749	0.235	0.053	0.134	0.014	0.183	0.126
70.00	0.910	0.214	0.758	0.244	0.053	0.141	0.015	0.183	0.126
73.34	0.924	0.218	0.765	0.254	0.053	0.147	0.016	0.183	0.126
76.67	0.937	0.221	0.771	0.263	0.053	0.154	0.017	0.183	0.126
80.00	0.947	0.223	0.773	0.272	0.053	0.161	0.017	0.183	0.126
83.34	0.956	0.225	0.778	0.278	0.053	0.164	0.018	0.181	0.124

showed that the relatively low power density core adopted provides flexibility in fuel management to achieve longer cycle lengths with relatively low CRF values, and thus favorable economics and good fissile use. This flexibility can benefit deployment opportunities to meet various needs of global utilities and markets.

The results of the analysis showed that within current regulatory limits on enrichment, 24-month cycles provide

an optimal trade-off between economic performance and fuel utilization while exhibiting reduced sensitivity to variations in the economic input parameters. Shorter cycle lengths allow for minor improvements in fuel utilization, but at the expense of economic performance and increased sensitivity to economic assumptions related to outages. Conversely, extending the cycle beyond 24 months does not yield significant economic benefits, with improved plant availability at the expense of fissile use.

The general trends indicate that, especially for longer cycles, adopting LEU+ fuel offers an opportunity to minimize the LCOE through a reduction in CRF and an increase in fissile use, relative to current enrichments. However, these benefits are not decisive and depend on resolving challenges related to increased fuel residence time and maximum pin burnup, beside the availability of LEU+ fuel.

This study underscores the nonnegligible influence of outage-related expenses and associated assumptions in determining the most favorable economic scenarios. Broader economic trends using the LRM have been identified using a wide range of bounding assumptions. More detailed evaluations are required to identify optimal market-specific strategies, including verifications with comprehensive core design and safety assessments.

Acknowledgments

A special thanks to Westinghouse and Vattenfall AB, which are supporting this work economically and with technical supervision.

Author Contributions

CRediT: **Flavio Ferella:** Data curation, Formal analysis, Investigation, Software, Validation, Visualization, Writing – original draft; **Marcus Seidl:** Conceptualization, Investigation, Methodology, Resources, Supervision, Writing – review & editing; **Fausto Franceschini:** Methodology, Resources, Supervision, Writing – review & editing; **Cecilia Gustavsson:** Supervision, Writing – review & editing; **Henrik Sjöstrand:** Formal analysis, Methodology, Supervision, Writing – review & editing; **Andreas Solders:** Project administration, Supervision, Writing – review & editing; **Jesper Kierkegaard:** Project administration, Supervision, Writing – review & editing.

Disclosure Statement

No potential conflict of interest was reported by the author(s).

Funding

This work was carried out within the framework of the Academic Industrial Nuclear Technology Initiative (ANitA) collaboration and has been financially supported by the Swedish Energy Agency under project number [52680-1]. It has also been supported by Uppsala University and the centre's industrial partners. This work was further supported by the Swedish Centre for Nuclear Technology and the Swedish Radiation Safety Authority [activity number 4530758].

ORCID

Flavio Ferella http://orcid.org/0009-0002-0661-8250

References

1. "Adavanced Reactor Information System: Status Report—AP1000," International Atomic Energy Agency, Vienna (2024); https://aris.iaea.org/Publications/20-02619E_ALWCR_ARIS_Booklet_WEB.pdf.
2. D. L. Stucker et al., "Levelized Cost of Electricity Evaluation Methodology Applied to High-Burnup 18 and 24-Month Fuel Cycles," *Proc. 2021 28th Int. Conf. on Nuclear Engineering*, *Vol. 2: Nuclear Fuels, Research, and Fuel Cycle; Nuclear Codes and Standards; Thermal-Hydraulics*, V002T05A019, Virtual, August 4–6, 2021, American Society of Mechanical Engineers (2021); https://doi.org/10.1115/ICONE28-66589.
3. "INPRO Methodology for Sustainability Assessment of Nuclear Energy Systems: Economics," Nuclear Energy Series NG-T-4.4, International Atomic Energy Agency, Vienna (2014); https://www-pub.iaea.org/MTCD/Publications/PDF/Pub1653_web.pdf.
4. L. M. Krall, A. M. Macfarlane, and R. C. Ewing, "Nuclear Waste from Small Modular Reactors," *Proc. Nati. Acad.Sci. USA*, **119**, *23*, e2111833119 (2022); https://doi.org/10.1073/pnas.2111833119.
5. M. Ouisloumen et al., "Paragon: The New Westinghouse Assembly Lattice Code," presented at the Int. Mtg. on Mathematical Methods for Nuclear Applications, Salt Lake City, UT, American Nuclear Society (2001).
6. M. J. Driscoll, T. J. Downar, and E. E. Pilat, *The Linear Reactivity Model for Nuclear Fuel Management*, American Nuclear Society (1990).
7. M. Egan, "Elements of Nuclear Reactor Fueling Theory," *Prog. Nucl. Energy*, **14**, *3*, 313 (1984); https://doi.org/10.1016/0149-1970(84)90026-X.
8. R. Woehlke and B. Quan, "Improvement of Linear Reactivity Methods and Application to Long Range Fuel Management," *Proc. U.S. Nuclear Regulatory Commission Mtg. on Advances*

in Reactor Physics and Core Thermal Hydraulics, p. 880, Kiamesha Lake, NY (1982).

9. F. Franceschini and B. Petrović, "Fuel with Advanced Burnable Absorbers Design for the IRIS Reactor Core: Combined Erbia and IFBA," *Ann. Nucl. Energy*, **36**, *8*, 1201 (2009); https://doi.org/10.1016/j.anucene.2009.04.005.
10. J. Bernstein, "SWU for You and Me," *arXiv:0906.2505 Rev. arXiv:0906.2505v1* (2009); https://arxiv.org/abs/0906.2505.
11. B. W. Dixon et al., "Advanced Fuel Cycle Cost Basis—2017 Edition," Idaho National Laboratory (2017); https://doi.org/10.2172/1423891.
12. "Nuclear Fuel Cycle Cost Basis Report," NUREG-2242, U.S. Nuclear Regulatory Commission, Washington, DC (2021); https://www.nrc.gov/docs/ML2117/ML21174A176.pdf.
13. "Appendix J to Part 50—Primary Reactor Containment Leakage Testing for Water-Cooled Power Reactors," *Code of Federal Regulations*, Title, 10, "Energy," Part 50, Washington, DC, U.S. Nuclear Regulatory Commission.
14. M. Bunn et al., "The Economics of Reprocessing vs Direct Disposal of Spent Nuclear Fuel," University of North Texas Libraries, Cambridge, MA, UNT Digital Library (2003); https://digital.library.unt.edu/ark:/67531/metadc786133/.